

Binary Galaxies in the Local Supercluster and Its Neighborhood

I. D. Karachentsev¹ and D. I. Makarov^{1,2}

¹*Special Astrophysical Observatory of the Russian AS, Nizhnij Arkhyz 369167, Russia**

²*Invited Researcher Observatoire de Lyon, St-Genis Laval Cedex, France 69561*

(Received May 22, 2008; Revised June 9, 2008)

We report a catalog of 509 pairs identified among 10403 nearby galaxies with line-of-sight velocities $V_{LG} < 3500$ km/s. We selected binary systems in accordance with two criteria (“bounding” and “temporal”), which require the physical pair of galaxies to have negative total energy and its components to be located inside the zero-velocity surface. We assume that individual galaxy masses are proportional to their total K -band luminosities, $M = L_K \times 6M_\odot/L_\odot$. The catalog gives the magnitudes and morphological types of galaxies and also the projected (orbital) masses and pair isolation indices. The component line-of-sight velocity differences and projected distances of the binary systems considered have power-law distributions with the median values of 35 km/s and 123 kpc, respectively. The median mass-to- K -band luminosity ratio is equal to $11M_\odot/L_\odot$, and its uncertainty is mostly due to the errors of measured velocities. Our sample of binary systems has a typical density contrast of $\delta\rho/\rho_c \sim 500$ and a median crossing time of about 3.5 Gyr. We point out the substantial fraction of binary systems consisting of late-type dwarf galaxies, where the luminosities of both components are lower than that of the Small Magellanic Cloud. The median projected distance for 41 such pairs is only 30 kpc, and the median difference of their line-of-sight velocities is equal to 14 km/s which is smaller than the typical error for radial-velocity (30 km/s). This specific population of gas-rich dwarf binary galaxies such as I Zw 18 may be at the stage immediately before merging of its components. Such objects, which are usually lost in flux-limited (and not distance-limited) samples deserve a thorough study in the HI radio line with high spatial and velocity resolution.

I. INTRODUCTION

*Electronic address: ikar@luna.sao.ru

This is the first paper of a series devoted to the study of the visible and dark mat-

ter within the nearby, but sufficiently representative volume of the Local Supercluster (LS) and its neighborhood, which is comparable to the size of a cosmological homogeneity cell. Over the past decade mass spectroscopic and photometric galaxy surveys—SloanDSS, 2MASS, 2dF, and 6dF—have been performed, which reshaped and refined our concepts about the large-scale structure of the Universe. However, the surveys performed within certain sky areas or in narrow strips out to redshifts $z \simeq 0.1\text{--}1.0$ proved to be insufficient to allow analyses of the structure and kinematics of small-scale features like the Local Group, since they did not include numerous dwarf galaxies because of their low luminosity. For example, in the Sloan Digital Sky Survey (SDSS) the mean distance between galaxies with measured line-of-sight velocities is equal to 9 Mpc, which exceeds the diameter of a typical cluster.

In recent years, considerable effort was focused on the study of the most nearby, so-called Local Volume (LV) of radius 10 Mpc, where more than 500 galaxies have been found. Most of these objects are dwarf systems with measured line-of-sight velocities, and about half of these galaxies already have individual distance estimates that are accurate to at least 10%, supported by observations made with the Hubble Space Telescope. The detailed 3D pattern of the distri-

bution of galaxies in the LV, where the density of galaxies with measured velocities is two orders of magnitude higher than the corresponding density for the SDSS, 2dF, and 6dF surveys, allowed the structure and kinematics of groupings to be studied on scale lengths 0.1–1 Mpc [1, 2, 3]. The contribution of the virial masses of nearby groups proved to be three-to-four times less than the average cosmological density, $\Omega_m = 0.27$. This inconsistency between the local and global Ω_m estimates can be due to poor statistics or to some specifics of our immediate neighborhood. An evident way for resolving this paradox consists in increasing the volume studied to make it include the entire Local supercluster and its immediate neighborhood. Tully [4, 5] was the first to successfully undertake such an analysis. He compiled a catalog and an atlas of nearby galaxies with line-of-sight velocities smaller than 3000 km/s. Tully's catalog contains a total of 2367 galaxies located inside the volume of diameter 82 Mpc, which is comparable to the volume of a cosmological homogeneity cell. Tully used the hierarchical dendrogram method to identify in this volume a total of 179 groups, which included 69% of all the galaxies considered. He then used the virial masses of these groups to infer a lower limit for the local mass density, $\Omega_{vir} = 0.08$, which proved to be three times smaller than the global value of $\Omega_m = 0.27$.

The amount of dark matter per unit luminosity of galaxies is known to increase from small groups to rich clusters. However, the virial regions of clusters contain only 5–10% of all galaxies, and about the same number of galaxies are associated with the unvirialized peripheral regions of these clusters. About half of all galaxies are members of groups like our Local Group, about one fourth of all galaxies reside in dispersed groups (clouds), and a total of 5–10% of all galaxies are located in the overall field. In such rather arbitrary and coarse partition groups of galaxies are the main contributors to the global mean mass density. However, the characteristic estimates of the masses of groups of galaxies differ by more than one order of magnitude. This circumstance emphasizes the need for further refinement of virial masses of groups of galaxies, which is great importance for cosmology.

Below we consider galaxies with line-of-sight velocities with respect to the Local Group $V_{LG} < 3500$ km/s. After excluding the region of strong absorption at Galactic latitudes $|b| < 15^\circ$ we fixed a total of 10403 galaxies in this volume and applied to them the criterion of identifying multiple systems.

In this paper we consider only binary galaxies, because the corresponding sample illustrates most clearly the specific features of the criterion employed. In our next papers we

plan to present the list of galaxy triplets and analyze the properties of groups with four to 400 members, describe our catalog of very isolated LSC galaxies, and specific features of the distribution of voids. Individual Tally–Fisher distances [6] are already available for about 1700 LSC galaxies [7]. We plan to use these data to analyze non-Hubble motions in the LSC in order to probe the distribution of dark matter on 3–10 Mpc scale lengths.

II. CRITERIA FOR SELECTING MULTIPLE SYSTEMS OF GALAXIES

Various algorithms have been suggested to identify groups of galaxies in a magnitude- or distance-limited sample. All these algorithms actually reduce to the following two main ones: percolation (the “friend of friend” method) and taxonometry (construction of a hierarchical tree).

Huchra and Geller [8] used the percolation method by joining galaxies into groups based on the condition that their projected mutual distances and line-of-sight velocity differences should be smaller than certain threshold values R_c and V_c . With $R_c = 0.52$ Mpc and $V_c = 600$ km/s the above authors grouped about 74% CfA galaxies. The resulting groups had a typical size of $R_H = 1.1$ Mpc, line-of-sight velocity dispersion of $\sigma_v = 208$ km/s, and an average virial mass

of $\lg(M_{vir}/M_\odot) = 13.5$. Many authors applied this method to different galaxy samples. One of the weak points of the method is freedom in the choice of two percolation parameters, R_c and V_c , whose variation affects substantially the characteristic sizes and masses of the groups and the percentage of galaxies found to be group members. In the percolation algorithm parameters R_c and V_c trace certain contrast of galaxy number density and overlooks many real groups in low-density regions, while clusterizing small unvirialized aggregates in high-density regions. Another disadvantage of the “friend of friend” methods manifest itself in the form of the strong dependence of group parameters on the distance D to the group. Numerous attempts aimed to reduce this dependence by introducing variable quantities $R_c(D)$ and $V_c(D)$ resulted in subjectively arbitrary choices. The most recent application of the percolation method to 2MASS [9] galaxies yielded 1258 groups and 1710 pairs of galaxies for a relative density contrast of $\delta\rho/\rho = 80$. In general, members of groups and pairs make up for a total of 36% and 17% of the entire sample. Groups with $n \geq 5$ elements have a projected radius of about 1 Mpc, line-of-sight velocity dispersion on the order of 200 km/s, and an average virial mass of $\lg(M_{vir}/M_\odot) \sim 13.5$. At the depth of the 2MASS sample ($D_{max} = 140$ Mpc) the con-

tribution of virial masses of groups identified using the percolation method is equal to only $\Omega_m = 0.10\text{--}0.13$. An examination of the list of these groups gives a rise to numerous questions. In particular, we do not understand why Eridanus+Fornax I is the most massive cluster complex instead of Virgo, which we know as the center of the Local Supercluster.

Tully [4, 5] and Vennik [10] used another, “taxonometric”, method to group galaxies into pairs in accordance with the maximal ratio of luminosity to cubed mutual distance (L_{ik}/R_{ik}^3). The resulting pair was substituted by a “particle” with the luminosity equal to the total of the galaxies and the search for maximal (L_{ik}/R_{ik}^3) was repeated. The process ended by the construction of a single hierarchical “tree” with branches containing the entire galaxy sample considered. Cutting the tree branches at a certain level of the contrast of volume density yielded a set of branches (groups) whose sizes and virial masses depended on the adopted density (luminosity) contrast. Tully [4] used the method of dendrograms to infer a characteristic group radius of 0.32 Mpc and the average line-of-sight velocity dispersion of $M_{vir}/L_B = 94M_\odot/L_\odot$, which proved to be substantially lower than the average ratio for groups of the Huchra–Geller [8] list. Practical applications of both the percolation and the dendrogram methods ignored individual

properties of galaxies by viewing them as indistinguishable particles. It is evident that the same threshold values R_c and V_c would be sufficient (and even redundant) for clustering a pair of dwarf galaxies and, at the same time, evidently insufficient to bind a pair of giant galaxies. Such inadequacy of the criterion distorts the estimates of virial masses.

III. CLUSTERIZATION ALGORITHM

Galaxies can be grouped into small systems with their individual properties taken into account by viewing two arbitrary galaxies as a virtual bounded pair [11]. We proceed from this evident premise and require that the difference V_{ik} of the space velocities of galaxies in physical pair and their mutual space distance R_{ik} obey the condition of negative total energy

$$\frac{V_{ik}^2 R_{ik}}{2GM_{ik}} < 1, \quad (1)$$

where M_{ik} is the total mass of the pair and G is the gravitational constant. We correct the squared velocity difference of the pair V_{ik}^2 for velocity measurement errors. However, observations give us only the line-of-sight projection of velocity V_{ik} and the sky-plane projection of R_{ik} . Therefore condition (1) must be supplemented by an additional constraint onto the maximum distance between

the components for fixed mass M_{ik} . The condition that the components of the pair are located inside the “zero-velocity” sphere [12] has the following form

$$\frac{\pi H^2 R_{ik}^3}{8GM_{ik}} < 1, \quad (2)$$

where H is the Hubble constant. Note that both conditions (1) and (2) are conservative with respect to projection factors, i.e., use of projected mutual velocities and distances in formulae (1) and (2) instead of the space velocities and distances does not exclude true (physical) pairs. However, these conditions do not prevent false (optical) pairs from getting into the catalog.

Our algorithm is actually a variant of the percolation method. We first identify all pairs satisfying conditions (1) and (2) and then group all pairs having a common component into a single entity. Finally, if we find a galaxy to be a satellite of several more massive galaxies, we link it to the most massive neighbor. In particular, a group may be a subgroup inside a more massive structure. In this sense, our algorithm combines the advantages of both the “friend of friend” method and hierarchical approach.

We determine the masses of galaxies from their -band IR luminosity assuming that all galaxies have the same “mass–luminosity” ratio:

$$M/L_K = \kappa(M_\odot/L_\odot), \quad (3)$$

where we set κ equal to 6. In our algorithm $\kappa = 6$ is actually the only more or less arbitrary quantity. We chose it based on the following assumptions. According to the data of Bell et al. [13], the average cosmic mass-to- K -band-luminosity ratio is equal to $0.95 \pm 0.27 M_{\odot}/L_{\odot}$, which agrees well with the results of the computations of Fukijita et al. [14]. According to the data compiled by Karachentsev and Kut'kin [15], for galaxies of the Local Volume the average ratio of the mass inside standard radius R_{25} to the integrated K -band luminosity is equal to $\langle M_{25}/L_K \rangle = 1.3 \pm 0.2$ in solar units, and this ratio remains almost constant and varies from 1.1 ± 0.2 for giant galaxies with the mean luminosity of $1.1 \times 10^{11} L_{\odot}$ to 1.5 ± 0.2 for dwarf galaxies with the mean K -band luminosity of $1.1 \times 10^7 L_{\odot}$ (the slight increase of $\langle M_{25}/L_K \rangle$ toward dwarf galaxies is evidently due to higher content of the gaseous component). Flat rotation curves observed for most of galaxies indicate the dominating role of the dark halo beyond the standard radius R_{25} . The most extended rotation curves inferred from the data of the 21-cm line emission reach out to $R_{max} = (3-6)R_{25}$ [16, 17, 18]. These R_{max} values correspond to the global ratio of $M/L_K \simeq 6M_{\odot}/L_{\odot}$ used in formula (3).

Note that we “trained” clusterization algorithm (1–3) by applying it to the de-

tailed 3D distribution of galaxies in the Local Volume. Choosing dimensionless parameter κ values in the $\kappa < 4$ interval drastically reduces the relative number of clusterized galaxies, whereas adopting $\kappa > 10$ results in grouping of galaxies into extended and evidently nonvirialized aggregates. With the value $\kappa = 6$ adopted in this paper the dwarf companions in known nearby groups are usually located inside the zero-velocity spheres around massive galaxies of the corresponding groups. Note also that the average virial mass-to-luminosity ratio $\langle M_{vir}/L_K \rangle = 17.5 \pm 3.6 M_{\odot}/L_{\odot}$ for eight groups of the Local Volume: Local Group, M81, CenA, M83, IC342, Maffei, LeoI NGC6946 (whose mean luminosity is $\langle L_K \rangle = 1.3 \times 10^{11} L_{\odot}$) is almost equal to the typical M_{vir}/L_K ratio that we inferred for small groups of the same luminosity inside the entire volume of the Local Supercluster. Guzik and Seljak [19] found a similar total mass-to- K -band luminosity ratio— $(17.0 \pm 2.9 M_{\odot}/L_{\odot})$ —for small groups and field galaxies with $\langle L_K \rangle \sim 0.8 \times 10^{11} L_{\odot}$ by analyzing effects of gravitational lensing, and this fact demonstrates the good agreement of the galaxy group mass estimates obtained by two independent methods.

IV. INITIAL OBSERVATIONAL DATA

Our main sources of the data on line-of-sight velocities, apparent magnitudes, morphological types, and other parameters of galaxies are the HyperLEDA¹ [20] and NED² databases. Note that these databases contain a substantial number of objects with erroneous line-of-sight velocities adopted from automatic sky surveys like 6dF. Cases of confusion of coordinates and velocities are rather common for galaxies located closely to each other on the celestial sphere. The apparent magnitudes and line-of-sight velocities in the SDSS survey often correspond to individual knots and associations in bright galaxies. These effects are very important for selecting of true close pairs of galaxies. We took these effects into account and made necessary corrections, where possible. This proved to be most time-consuming part of our work. Because the databases are permanently updated with new (and sometimes erroneous) data, it is necessary to repeat the correction of information. That is why we fixed the sample of initial data as it was in mid-2006 (i.e., June, 2006).

We independently found optical identifications for many *HI* sources of the HIPASS

survey by refining their coordinates and determining the apparent magnitudes and morphological types of galaxies [21]. We examined many dwarf galaxies, especially those with low surface brightness, on the DSS digital images in order to find their principal parameters. The typical error of our visual estimates of galaxy magnitudes is about 0.5^m , and the average error of the inferred type is about ± 2 in the numeric scale employed by de Vaucoulers in the RC2 catalog [22]. The best indicator of the baryonic mass of a galaxy is known to be its infrared magnitude, which depends only slightly on the amount of dust and the number of young stellar complexes. Thus we adopted the longest-wavelength, *K*-band ($\lambda = 2.16 \mu\text{m}$) part of the all-sky 2MASS [23, 24] as our main source of photometry. We converted the estimates of galaxy magnitudes in other optical (*B, V, R, I*) and near-infrared bands (*J, H*) into the *K*-band magnitude using synthetic galaxy colors of Bizzoni [25] and Fukujita et al. [26]. The greatest amount of photometric data is available in the *B*-band. We use the following relations between the *B-K* color excess and morphological type discussed by Jarett et al. [24] and Karachentsev and Kut'kin [15] :

$$\langle B-K \rangle = +4.10, \text{ for galaxies of types } T \leq 2 \text{ (i.e., E, S0, and Sa), which are dominated by bulges,}$$

¹ <http://leda.univ-lyon1.fr>

² <http://nedwww.ipac.caltech.edu/>

$\langle B - K \rangle = +2.35$ for late-type galaxies $T \geq 9$ (i.e., Sm, Im, Irr), and

$$\langle B - K \rangle = 4.60 - 0.25 \times T \text{ for intermediate-type } (T = 3-8) \text{ objects.}$$

Note that due to the short exposures the 2MASS survey proved to be insensitive to low-surface brightness and blue galaxies. For about one thousand dwarf and spheroidal galaxies recently discovered by Karachentseva et al. [27, 28] in the volume of the Local Supercluster, only eye-estimated B -band magnitudes are available, which we converted into the K -band magnitudes using the method described above. Despite the lack of good photometry for these objects, gas-rich dIr galaxies have accurate 21-cm line radial velocities and they are important “test particles”. Due to the low luminosities of dwarf galaxies, large errors of estimated magnitudes have virtually no effect on the results of clusterization performed using our algorithm.

We collected all the line-of-sight velocity measurements available in the HyperLEDA and NED databases for galaxies in the Local Supercluster and its neighborhood. We excluded unreliable and inaccurate measurements, which velocity-measurement error exceeds 75 km/s. In automatic surveys (SDSS, 2dF, and 6dF) we also excluded the measurements with velocities smaller than 600 km/s, because they mostly represent Milky-Way stars projected onto distant galaxies. If sev-

eral line-of-sight velocity measurements were available for a galaxy, we chose the median one, the velocity error was estimated as the dispersion of all measurements with the exclusion of the outliers.

Our initial sample cleaned from unreliable and doubtful cases contained a total of 10403 galaxies with the line-of-sight velocities $V_{LG} < 3500$ km/s, located at the Galactic latitudes $|b| > 15^\circ$. For all these galaxies the apparent magnitudes and morphological types have been found. To prevent the distortion of the clusterization process at the boundary of the volume considered, we also use the data on the galaxies located in the boundary regions with $10^\circ < |b| < 15^\circ$ and with $3500 < V_{LG} < 4000$ km/s, because they may contain some of the members of galaxy groups with high virial velocities. Grouping criteria (1–3) allowed us to identify within the Local Supercluster volume a total of 1018 galaxies belonging to binary systems.

V. THE CATALOG OF 509 NEARBY GALAXY PAIRS

The Table contains the binary galaxies that we identified using our criteria. The first column gives the number of the pair in the catalog. The second column gives the name of the galaxy or its number in the well-known NGC, IC, UGC, CGCG, ESO, PGC,

and DDO catalogs or in the 2MASS, 6dF, APMUKS, SDSS, IRAS, and other sky surveys as given in the NED. Note that for practical reasons we omit the coordinate part of the galaxy name used in surveys. The third column gives the galaxy coordinates for the epoch of 2000.0. The fainter component of the pair follows the primary component and the pairs are sorted in right ascension. Columns (4) and (5) give the line-of-sight velocity of the galaxy (in km/s) with respect to the centroid of the Local group and its standard error, respectively. Columns (6) and (7) give the coded morphological type and the apparent K -band magnitude corrected for Galactic extinction according to Schlegel et al. [29], respectively. Column (8) gives the projected separation between the galaxies in kpc. Column (9) gives the logarithm of the total K -band luminosity of the pair. Columns (10) and (11) give the orbital mass-to-luminosity ratio with and without velocity measurement correction, respectively. We compute the mass by the following formula [30]

$$M_p = \frac{16}{G\pi} \Delta V^2 R_{\perp} \quad (4)$$

using the component line-of-sight velocity difference and projected linear separation. We compute the distance to the pair from the average line-of-sight velocity with respect to the centroiod of the Local group

with the adopted Hubble-constant value of $H = 73$ km/s/Mpc. Column (12) gives the logarithm of the smallest of the values given by criteria (1) and (2) for the given pair with respect to the surrounding galaxies. The higher is this quantity, the greater is the degree of isolation of the considered pair. A close-to-zero value implies that the pair is at the threshold of the formation of a bigger structure (“capturing” of a new member or “joining” other groups). We compute the total luminosity of the pair assuming that the absolute magnitude of the Sun is $K_s = 3.28^m$ [31]. We omit the negative unbiased estimated of the orbital mass for the pairs with line-of-sight velocity differences smaller than the corresponding measurement errors.

VI. DISTRIBUTIONS OF THE PRINCIPAL PARAMETERS OF THE PAIRS

The fraction of galaxies that are members of binary systems in the Local Supercluster and its neighborhood is about 10%, which is somewhat lower than the corresponding values 12–17%, according to the data of Huchra and Geller [8], Crook et al. [9], Magtesyan [32], and Gourgoulhon et al. [33]. Figure 1 shows the distribution of the mean line-of-sight velocity of the pairs. The median

of this distribution is equal to 2389 km/s. Figure 2 shows the map of the distribution of pair centers on the sky in equatorial coordinates. The region of strong Galactic absorption is shown by gray color. It is obvious from this map and from 3D distribution (Fig. 3) that the pairs do not reveal clear large scale structure. However, on short scale lengths in the vicinity of 1 Mpc, the pairs exhibit excess of mutual association compared to uniform random distribution. The pairs 21+22 and 194+195 are examples of such close associations.

Figure 4 shows the distribution of the line-of-sight velocity difference between the satellite and the primary component of the pair. The distribution has quite symmetric shape with a mean difference of -1 ± 3 km/s, which indicates that our sample exhibits no excess of positive velocities discussed by Arp [34] in cases of the companions of M31 and other galaxies. The root-mean-squared velocity difference for the components of 509 pairs is equal to $\sigma_v = 62$ km/s. Note that in the vicinity of zero the distribution is much sharper than a Gaussian. Note also that for about 60% of all pairs the velocity difference is smaller than its error of measurement. For such pairs unbiased estimates of orbital masses are negative and we do not give them in Column 11 of the table. Taking into account broadening of distribution by errors,

the true distribution in Fig. 4 must have an even sharper peak at zero velocity difference. Note the measurement errors of velocity must be reduced several times to improve the estimation of mean mass of pair.

Figure 5 shows the distribution of the projected linear separation between the components in 509 pairs. The median and mean separations are equal to 123 and 177 Mpc, respectively, and the separation in the widest pairs reaches 1 Mpc. In general, the population of binary galaxies outlines fairly well the linear size of a typical dark halo in the Λ CDM model. The distribution $N(R_{\perp})$ can be fitted by a power law with exponent an $\alpha = -1.1$. Figure 6 shows the two-dimensional distribution of the line-of-sight velocity difference and projected separation between the components of the pairs in logarithmic scale. Despite the strong effect of projection factors, pairs show a tendency toward a decrease of ΔV with decreasing separation between the components, however, the slope of the regression line (the dashed line) is very close to zero and the line differs significantly from the Keplerian law (the solid line). This envelope corresponds to values $\Delta V = 121$ km/s and $R = 750$ kpc, which is close to Andromeda and Milky Way as wide pair of galaxies. Note that normalization of ΔV by the total luminosity of the pair makes the slope of the regression line closer to the Keplerian value.

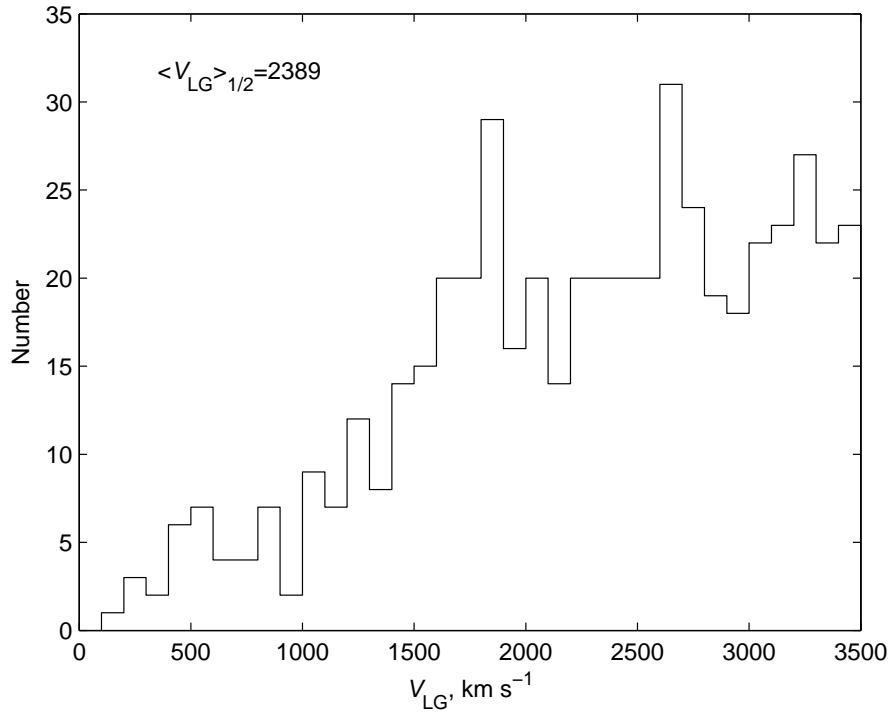


Figure 1: The distribution of the average line-of-sight velocities of pairs with respect to the Local Group.

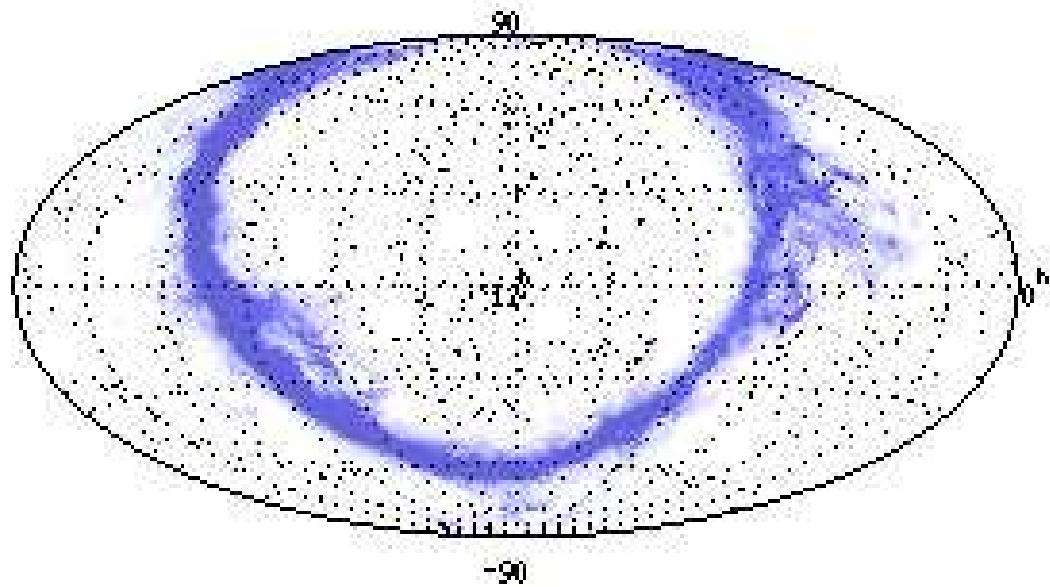


Figure 2: The celestial distribution of pairs in the Local Supercluster in equatorial coordinates. The clumpy gray region indicates the domain of strong Galactic absorption.

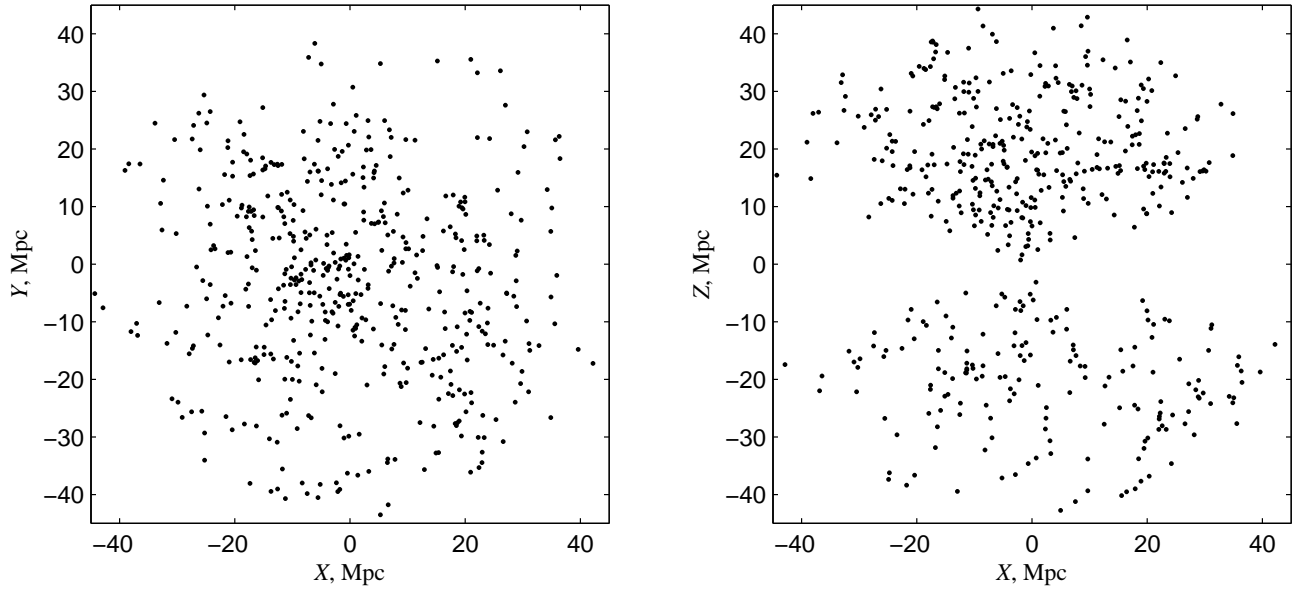


Figure 3: Projected distribution of pairs in the Local Supercluster in Cartesian coordinates.

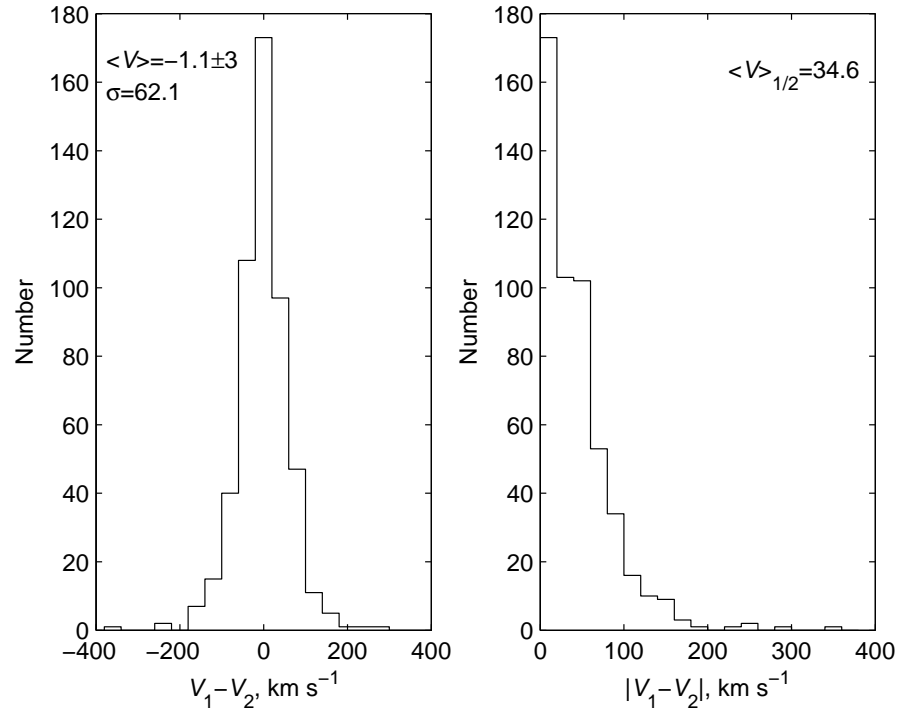


Figure 4: The distribution of the companion minus primary line-of-sight velocity difference.

The left- and right-hand panels in Figure 7 show the distributions of the visual (left) and absolute (right) K -band magnitudes of the bright (1) and faint (2) components of the

pairs. Both distributions fill more or less uniformly a wide sector of possible values over 10-magnitude range. About 40% of all pairs differ in luminosity less than a

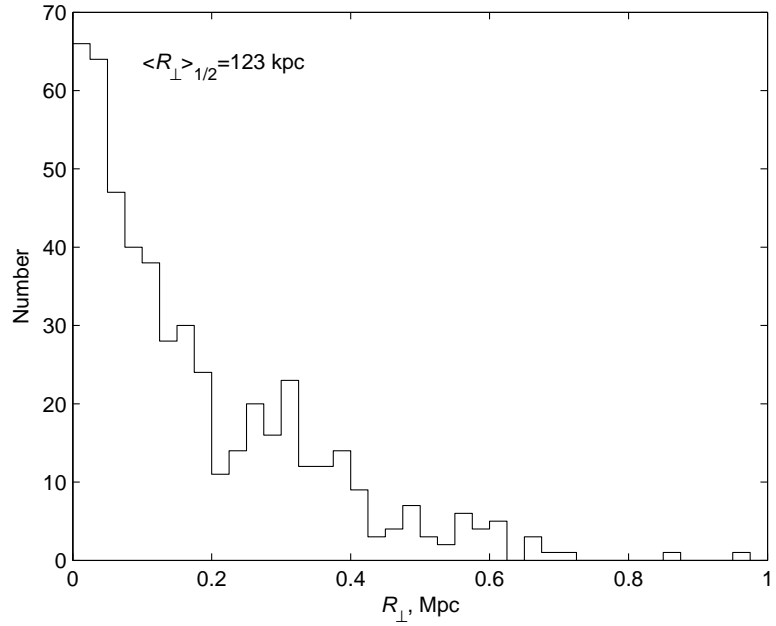


Figure 5: The distribution of the projected separation between the components in the pairs of the Local Supercluster.

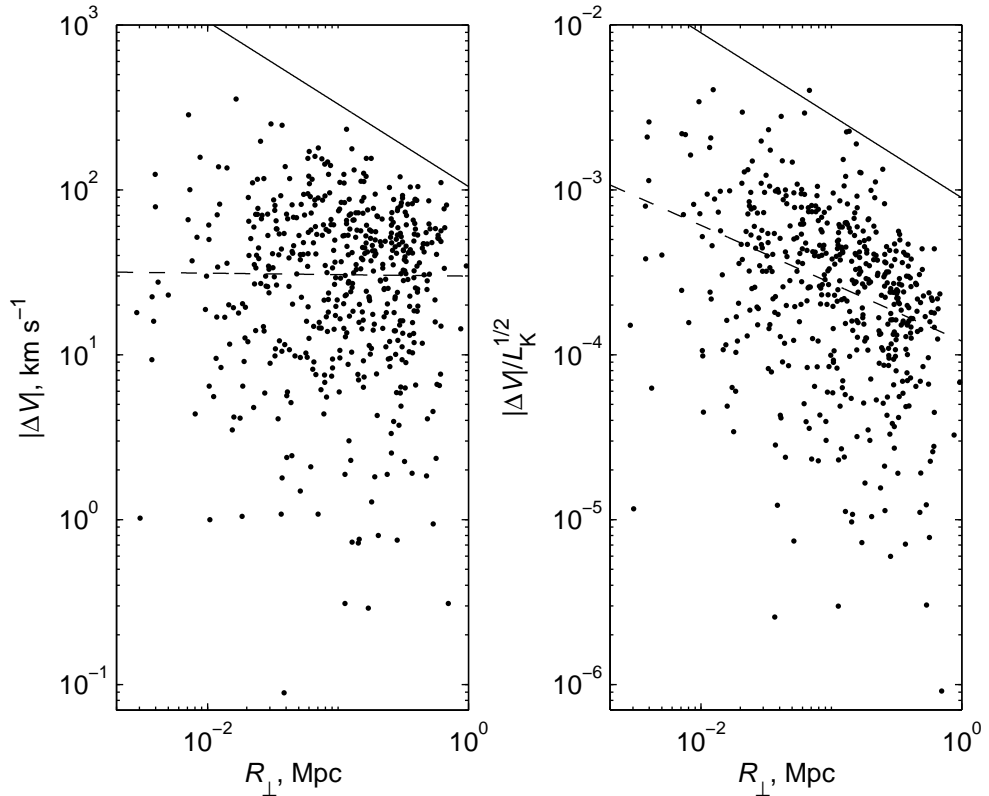


Figure 6: The distribution of the line-of-sight velocity difference and projected separation for the pairs of the Local Supercluster.

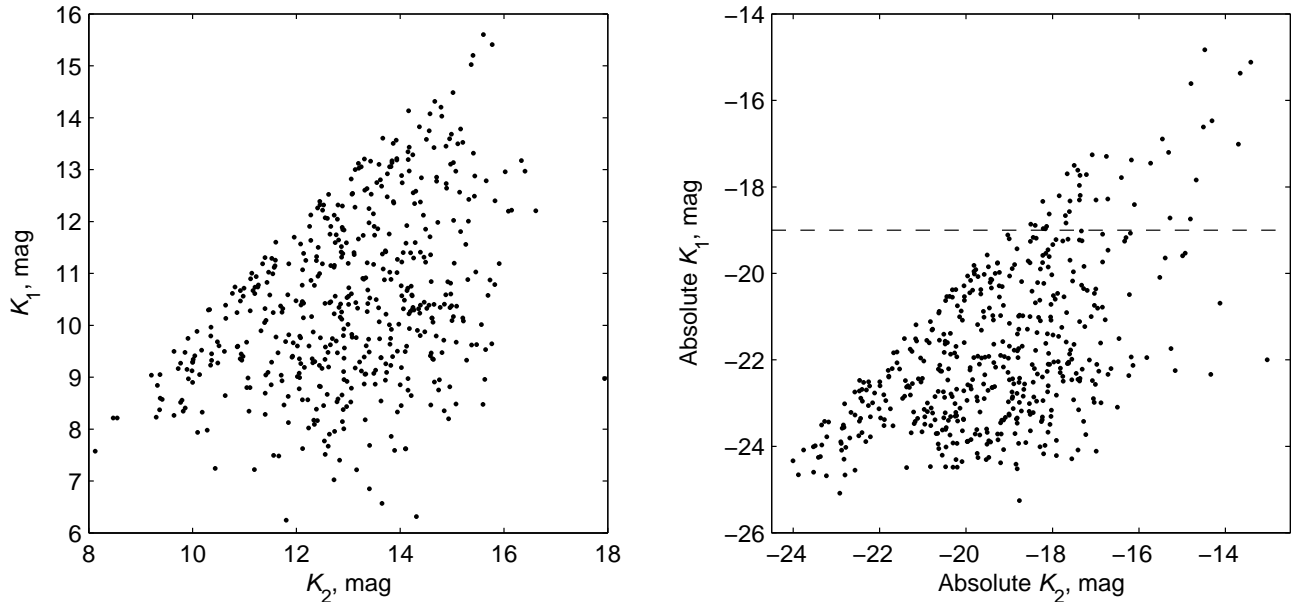


Figure 7: Distribution of the apparent (left) and absolute (right) K -band magnitudes of the bright (1) and faint (2) components in the Local Supercluster.

10 times. At the same time, there are galaxies, e.g., NGC 3044, NGC 2683, and NGC 3621, with dwarf companions that are 7–10 magnitudes fainter than the primary component. The special interest are drawn by the pairs located in the top right corner of the right-hand panel in Fig. 7. The dashed line in this panel corresponds to $M_K = -19.0$ (the luminosity of the SMC). Pairs that are located above this line have both components that are dwarf galaxies. There are total of 41 pairs like UGC 5272 and its companion (pair No. 159), which are located in the domain of lower-than-SMC luminosity. The pair of metal-poor BCD dwarfs SAO0822+3545 and SDSSJ0825+3532 (pair No. 113) studied by Cnehtagur et al. [35] is another example. Al-

most all these binary dwarfs are gas rich and contain young blue stellar population. The average component line-of-sight velocity difference for these pairs is equal to only 25 km/s, and the median and mean projected separations are equal to 30 and 42 kpc, respectively. These pairs of blue dwarfs with considerable reserves of gas and active star formation may be a sort of small multiple systems at a stage close to component merger. On the other hand, Tully et al. [36] pointed out the presence in the Local Volume of groups which exclusively consist of dwarf galaxies. Note that old percolation criteria proved to be insensitive to multiple dwarf systems. They were discovered as a result of, among other things, in-depth analysis of the

population of the Local Volume and of use a more refined algorithm for group searching. It is evident that *HI*-observations with high angular resolution would be a promising method for analyzing the kinematics and evolutionary status of dwarf pairs pairs and groups.

Figure 8 shows the distribution of the morphological types of the bright (1) and faint (2) components of 509 pairs. On the average, the primary galaxy have an earlier type ($\langle T_1 \rangle = 3.8$) than its companion ($\langle T_2 \rangle = 6.9$). This fact is easy to explain by the well-known correlation between the luminosity and morphological type of galaxies. The lines of direct and reverse regression in Fig. 8 point out a weak correlation between the morphological types of the components, which also can be due to the luminosity effect.

Figure 9 shows the distribution of estimated orbital masses and orbital mass-to-luminosity ratios for galaxy pairs inferred in accordance with formula (4). The median mass of the pairs is $1.5 \times 10^{11} M_\odot$, and the median mass-to-luminosity ratio is $11.3 M_\odot / L_\odot$, which is almost twice the $\kappa = 6$ value that we adopt for individual galaxies. However, these mass estimates are statistically biased. We already pointed out above that the line-of-sight velocity difference is smaller than its standard error for more than half of all pairs. To obtain an unbiased mass

estimate, we must substitute $(V_{12}^2 - \sigma_1^2 - \sigma_2^2)$ for V_{12}^2 in formula (4). In this case mass estimations become negative for 60% of the pairs and the median mass-to-luminosity ratio also becomes negative ($-3 M_\odot / L_\odot$). The distributions of M and M/L for the pairs corrected to for velocity measurement errors are shown in gray, but they represent only the domain of positive masses. All these data illustrate the fact that the accuracy of line-of-sight velocities measured in modern optical spectroscopic galaxy surveys (2dF, SDSS, 6dF), which is about 50 km/s, is clearly insufficient to compute a bona fide average mass of galaxy pairs. Obviously the special observations of binary galaxies are needed to reduce the velocity errors down to 5–10 km/s.

Figure 10 shows how the line-of-sight velocity difference, projected separation between the components, and the orbital mass-to-luminosity ratio of binary galaxies vary with heliocentric distance. It is evident that in our sample the fraction of pairs consisting of two dwarf components decreases appreciably toward the outskirts of the volume considered. However, the average dynamical parameters of the ensemble of galaxy pairs vary little with distance. This fact again demonstrates the advantage of our criterion, which takes individual properties of galaxies into account.

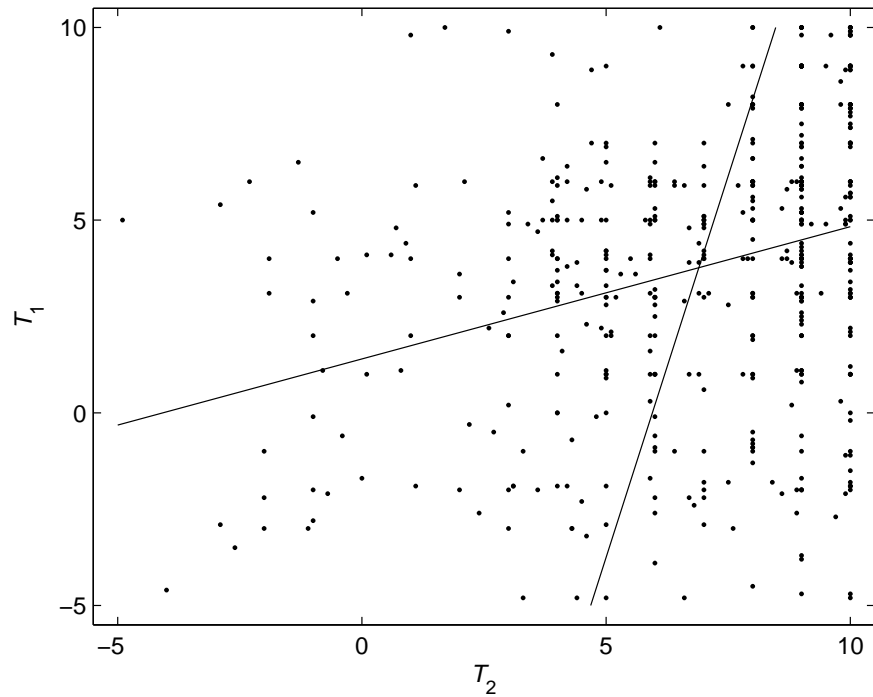


Figure 8: Distribution of the types of the bright (1) and faint components. The lines show the direct and inverse regression

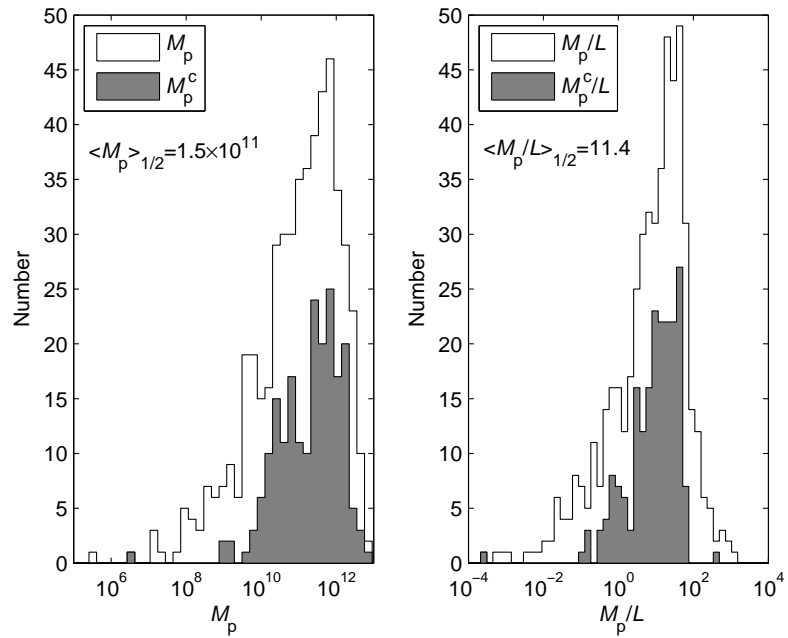


Figure 9: Distribution of estimated orbital masses and orbital mass-to-luminosity ratios for the pairs of the Local Supercluster.

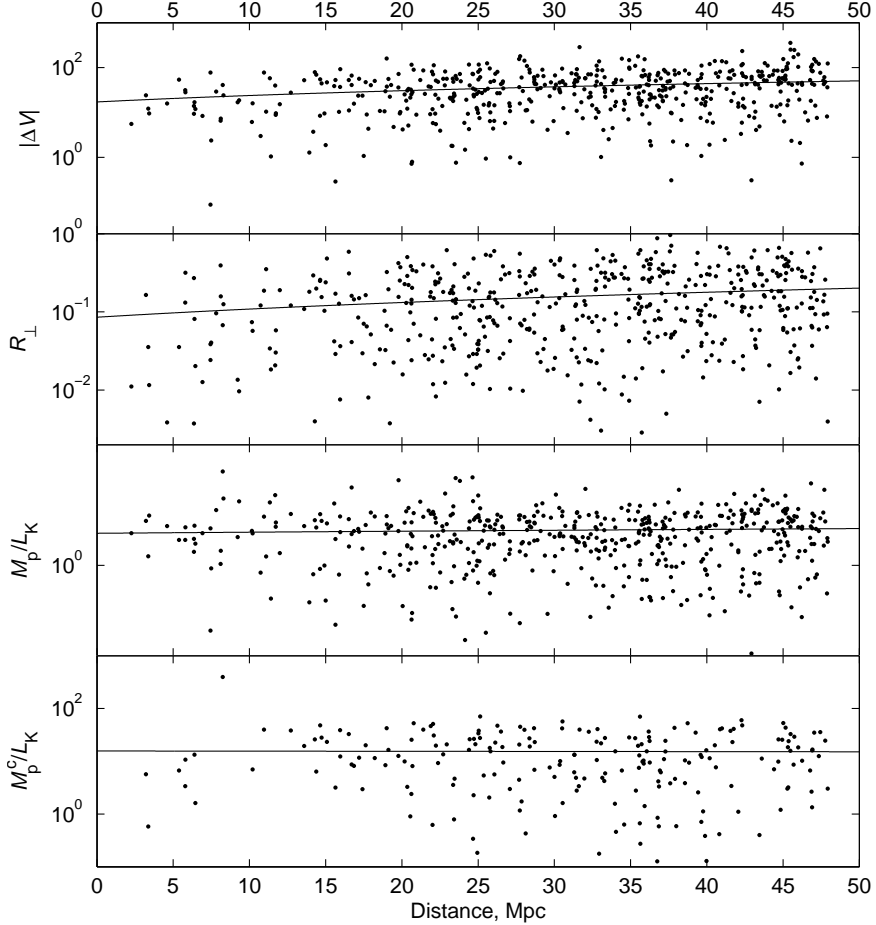


Figure 10: Characteristic diagrams showing how the properties of identified galaxy pairs vary with distance.

VII. COMPARISON WITH OTHER SAMPLES OF GALAXY PAIRS

The most detailed study of binary galaxies was performed by Karachentsev [37]. He compiled a catalog of 603 isolated Northern-sky pairs with components brighter than $B = 15.7^m$ (they are denoted as KPG in the NED database). These pairs were identified on the condition that they are isolated with respect to nearby projected galaxies without invoking line-of-sight velocity data. Later Reduzzi

and Rampazzo [38] used the same criterion to identify a total of 409 pairs in the Southern sky (these pairs are denoted as RR in the NED database). The isolation condition favored the identification of closer binary systems with brighter components. The characteristic depth of the KPG sample is 6350 km/s, which is substantially greater than the Local Supercluster sample considered in current paper. After taking into account various selection effects in the catalog of isolated

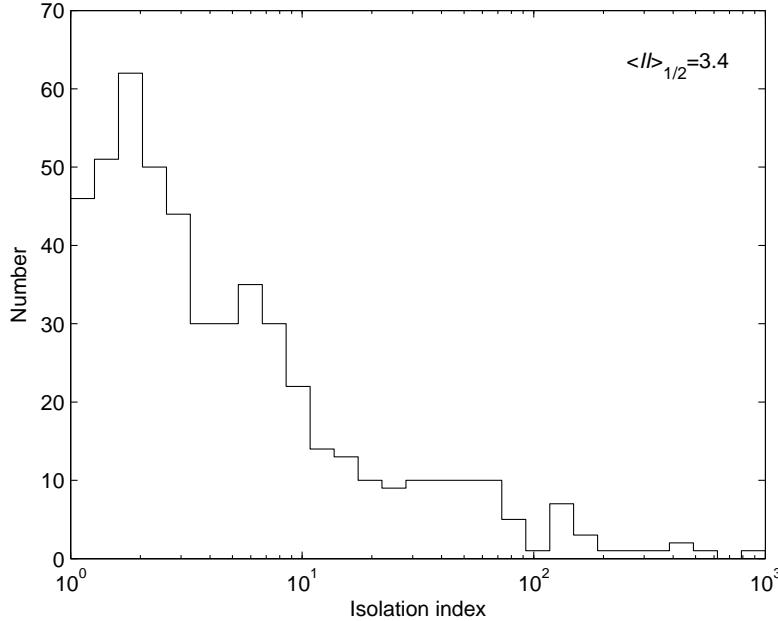


Figure 11: Distribution of the index of isolation of the pairs of the Local Supercluster with respect to neighboring galaxies.

pairs we estimate the fraction of galaxies in binary systems to be $12 \pm 2\%$. The KPG pairs with their order-of-magnitude higher luminosities (about $1.3 \times 10^{11} L_\odot$ if transformed into the K -band values) have large line-of-sight velocity differences, $\langle V_{12} \rangle = 120$ km/s. With the average component separation of only $\langle R_\perp \rangle = 40$ kpc, isolated pairs have a moderate orbital mass-to-luminosity ratio of $\langle M/L_B \rangle = 7.8 M_\odot/L_\odot$ and almost do not show evidence for dark halo on these lengths.

Our list contains a total of 16 pairs located within the rather thoroughly studied Local Volume. In cases where individual distances have been measured for components of nearby pairs these distances confirm the rela-

tive closeness of the pair members. However, the distances of the NGC 4449 and UGC 7577 galaxies (pair No. 281) (4.21 and 2.54 Mpc, respectively) indicate that these galaxies are just accidentally located along the same line of sight. Despite the small line-of-sight velocity difference (252 km/s and 240 km/s) and rather isolated location ($II = 2.3$) these members of the CVnI cloud cannot be viewed as an isolated physical pair.

Among the isolated pairs of the KPG catalog there are several known nearby pairs, in particular, NGC 5194 + NGC 5195 (M51) and NGC 672 + IC 1727. Although our criterion (1–3) clusterizes these galaxies, it nevertheless changes their status from pairs to groups, due to the presence of other dwarf

companions. Note that the properties of multiple galaxies identified using a certain criterion in the Local Volume differ from the corresponding properties of multiple galaxies found in deep samples due to the decreasing detection rate of dwarf objects with distance. That may be why the fraction of galaxies in binary systems, 12–17%, in about 100 Mpc deep samples is somewhat higher than in the Local Supercluster (10%) or Local Volume (7%).

VIII. CONCLUSIONS

We identified the galaxy pairs that we included in our catalog without using the condition of isolation. Therefore, as new dwarf galaxies are found in the volume of the Local Supercluster and new line-of-sight velocity measurements are made for galaxies located in the vicinity of the pairs, the list of pairs will be updated by including new objects and some pairs will be promoted to a higher multiplicity category. However, our sample still gives a correct idea about the kinematics of the smallest, most simple systems within the 95-Mpc diameter volume. About 40% of the considered pairs have dimensionless parameters $II > 5$, which allow us to treat these objects as sufficiently isolated systems (Fig. 11). With the median mass of the pair, $1.5 \times 10^{11} M_\odot$, and median projected compo-

nent separation of $R_\perp = 123$ kpc, the typical density contrast in the ensemble of our pairs is $\delta\rho/\rho_c \sim 500$ in the units of critical density. At such contrast systems of galaxies can be considered to be dynamically detached from Hubble flow. On the other hand, with the median absolute value of the component line-of-sight velocity difference of 35 km/s and with the median projected separation of 123 kpc, a typical pair of our catalog is characterized by the “crossing time” of 3.5×10^9 yr. Hence the components of a typical pair could make about of four turns about the common mass center.

The use of the new clusterization algorithm, which takes into account individual properties of galaxies, allowed us to discover a surprisingly large number of pairs consisting of dwarf galaxies. Many components of these systems, which are located far from normal galaxies, are rich in gas and are characterized by active star formation. Such binary dwarf galaxies (for instance, IZw18) have been known long ago. Among of them the galaxies with very low metallicity [39] occur quite often. Our list of galaxy triplets with velocities $V_{LG} < 3500$ km/s also contains triple systems of dwarfs with blue components. Many properties of our systems of dwarf galaxies do not differ from the corresponding properties of associations of nearby dwarfs as described by Tully et al. [36]. The

closest example of the objects of this population is located at the boundary of the Local group and includes NGC 3109, Sex A, Sex B, and Antlia. The mutual velocities of these “dark groups” are equal to only 10 km/s, i.e., they are comparable to velocity measurement errors. The evolutionary status of multiple dwarf galaxies still remains totally unclear. According to the results of numerical simulations performed by Bekki [40], the evolution of such dwarf systems with extended gaseous envelopes may be governed by their consequent mergers triggering the star-formation bursts. We consider mass 21-cm line observations of these objects on aperture synthesis radio telescopes with a resolution of about 1 km/s is very perspective.

APPENDIX

Table I: **Table.** Catalog of binary galaxies in the Local Supercluster and its neighborhood.

No.	Name	J2000.0	V_{LG} km s $^{-1}$	\pm	T	K mag	R_\perp kpc	$\log L$ L_\odot	$\frac{M}{L_K}$ \odot	$\frac{M^c}{L_K}$ \odot	$\log(II)$
1	NGC7820	J000430.8+051201	3252	39	1	9.60	507	10.81	30.9	25.6	0.30
	UGC00027	J000428.8+055050	3310	5	6	12.25					
2	6dF...	J000432.0–220503	3154	74	10	13.05	217	9.55	320.8		1.41
	ESO538–021	J000545.9–220442	3220	10	6	13.80					
3	UGC00132	J001400.9+125746	1896	9	8	12.85	72	9.08	15.1	5.7	0.78
	PGC138138	J001354.2+124827	1910	5	10	14.70					
4	ESO078–022	J002056.8–635126	1632	20	4	11.18	226	9.64	37.5		0.88
	6dF...	J001636.1–641138	1608	74	9	12.50					
5	UGC00260	J002702.9+113502	2337	5	6	10.33	23	10.21	5.8	3.4	1.67
	CGCG...	J002653.2+113424	2277	20	5	13.18					
6	ESO079–003	J003202.2–641512	2474	13	3	9.01	83	10.82	32.4	28.3	1.85
	ESO079–002	J003201.1–642325	2622	27	7	12.02					
7	UGC00320	J003230.9+023427	2541	5	6	12.88	144	9.29	4.4		2.14
	APMUKS...	J003145.4+024253	2548	20	9	15.44					
8	NGC0148	J003415.5–314710	1842	17	-2	9.05	232	10.63	5.4		0.25
	IC1554	J003307.4–321530	1814	43	-1	10.14					
9	NGC0255	J004747.3–112807	1694	15	4	9.66	174	10.23	5.8	3.6	0.81
	DDO005	J004603.4–113020	1716	5	9	11.94					
10	NGC0357	J010321.9–062021	2515	16	0	8.43	269	11.02	1.0	0.6	0.93
	MCG...	J010508.6–061646	2533	5	9	12.97					
11	NGC0424	J011127.7–380500	3455	7	0	9.12	372	11.17	5.1		0.74
	NGC0438	J011334.2–375406	3414	26	3	9.99					
12	NGC0428	J011255.7+005854	1287	5	9	9.37	65	10.07	0.5		1.99
	UGC00772	J011339.4+005228	1296	6	10	13.63					
13	NGC0473	J011955.1+163241	2317	5	0	9.53	138	10.51	5.5	4.7	0.92
	LSBC...	J011947.4+164725	2350	6	10	15.65					
14	UGC00903	J012147.8+173533	2697	7	4	9.38	355	10.70	1.4	0.6	0.40
	UGC00883	J012101.0+170424	2684	5	10	13.63					
15	UGC00964	J012435.1+074316	2884	6	3	11.89	220	9.89	41.7	34.9	0.41
	VV730...	J012319.3+074747	2849	8	10	12.88					
16	LSBC...	J013029.0+024955	2240	10	5	13.57	60	9.09	9.1		0.11
	UGC01075	J013002.5+025109	2227	6	8	13.93					
17	NGC0578	J013029.1–224002	1645	5	5	8.58	44	10.57	9.3		0.47
	2MASX...	J013011.9–224545	1563	74	4	12.80					
18	NGC0573	J013049.3+411526	3028	5	5	11.07	235	10.26	4.9	3.4	1.94

Table I: **Table.** (Contd.)

No.	Name	J2000.0	V_{LG} km s $^{-1}$	\pm	T	K mag	R_\perp kpc	$\log L$ L_\odot	$\frac{M}{L_K}$ \odot	$\frac{M^c}{L_K}$ \odot	$\log(H)$
	UGC01070	J012959.9+405826	3046	5	6	12.12					
19	UGC01102...	J013229.6+043607	2092	29	6	11.30	30	9.74	6.9		0.06
	UGC01105	J013239.9+043830	2125	43	10	14.26					
20	NGC0613	J013418.2–292506	1470	8	4	7.02	503	11.12	4.3	3.3	0.68
	ESO413–007	J012759.3–290512	1501	8	–1	12.73					
21	NGC0632	J013717.5+055240	3301	12	–2	10.08	496	10.58	113.2		0.38
	UGC01137	J013512.8+053022	3216	75	10	15.22					
22	NGC0645	J014008.7+054336	3441	5	3	10.15	112	10.66	8.1	6.7	0.49
	UGC01172	J013938.5+054658	3389	12	8	12.13					
23	NGC0676	J014857.3+055427	1630	6	1	9.04	180	10.68	14.1	13.5	0.39
	NGC0693	J015030.9+060843	1686	6	0	9.21					
24	NGC0723	J015345.7–234528	1486	5	4	10.30	227	9.81	26.1	9.9	1.30
	ESO477–012	J015345.7–230650	1460	10	10	14.27					
25	NGC0779	J015942.3–055747	1461	5	3	8.09	421	10.68	13.6	12.6	1.30
	UGCA024	J020431.4–061156	1425	5	9	12.35					
26	NGC0821	J020821.1+105942	1862	18	–5	7.86	537	10.98	0.0		0.91
	kkh008	J021227.4+101959	1861	5	10	13.83					
27	NGC0851	J021112.1+034647	3208	38	–1	11.02	59	10.43	62.3	53.0	1.18
	IC0211	J021108.0+035109	3363	23	6	11.47					
28	NGC0853	J021141.2–091822	1615	34	9	10.44	243	9.86	3.5		1.01
	MRK1025	J020959.7–085011	1624	14	9	13.15					
29	NGC0865	J021615.1+283559	3175	8	5	10.22	304	10.51	0.3		2.47
	UGC01753	J021631.8+281213	3170	6	10	14.17					
30	NGC0895	J022136.5–053117	2338	5	6	9.40	22	10.59	8.2		0.14
	NGC0895a	J022145.2–053208	2448	75	9	13.86					
31	NGC0922	J022504.4–244717	3052	9	6	10.02	101	10.59	17.3		1.90
	2MASX...	J022430.0–244444	3126	74	4	12.99					
32	NGC0986	J023334.4–390242	1876	36	2	7.77	177	11.04	4.9		1.05
	ESO299–011	J023534.7–390131	1926	74	5	12.54					
33	IC0239	J023627.9+385812	1096	5	6	8.75	238	10.16	0.1		0.47
	NGC1023C	J024039.6+392247	1094	5	10	14.74					
34	NGC1090	J024633.9–001449	2809	5	4	9.19	389	10.80	54.7	43.1	0.54
	UGCA042	J024852.7–002103	2722	20	10	14.03					
35	NGC1140	J025433.6–100140	1508	5	9	10.49	204	9.77	0.0		0.30
	6dF...	J025333.5–103208	1509	74	10	13.54					
36	MCG...	J030031.8–154411	1506	55	7	10.77	143	9.74	0.0		0.63
	2MASX...	J030042.9–160752	1507	29	9	12.11					
37	NGC1172	J030136.1–145012	1645	8	–4	9.19	239	10.36	5.1		0.17

Table I: **Table.** (Contd.)

No.	Name	J2000.0	V_{LG} km s $^{-1}$	\pm	T	K mag	R_\perp kpc	$\log L$ L_\odot	$\frac{M}{L_K}$ \odot	$\frac{M^c}{L_K}$ \odot	$\log(II)$
	IRAS...	J030307.5–151932	1625	25	9	12.16					
38	UGC02497	J030207.7+290623	3265	5	8	11.31	297	10.11	6.2		2.94
	UGC02488	J030143.2+284413	3280	8	10	14.46					
39	NGC1196	J030335.2–120435	3371	22	–2	9.60	111	10.90	25.4	18.5	0.62
	IC0285	J030406.2–120056	3246	35	3	10.87					
40	NGC1201	J030408.0–260411	1609	20	–3	7.67	312	10.95	9.8	9.3	0.26
	ESO480–025	J030350.5–251620	1657	5	9	12.61					
41	LCRS...	J031049.7–414757	1253	74	9	12.92	41	8.76	379.6		0.24
	LCRS...	J031059.2–413940	1186	26	9	13.75					
42	NGC1253	J031409.0–024923	1723	6	6	9.23	27	10.42	16.7	16.4	1.23
	NGC1253A	J031423.3–024803	1840	8	9	12.45					
43	2MASX...	J031729.7–080843	2054	26	5	13.05	173	9.25	14.8		1.72
	SDSS...	J031829.0–075331	2065	5	8	13.25					
44	NGC1320	J032448.7–030232	2719	45	1	9.34	17	10.90	0.1		0.30
	NGC1321	J032448.6–030056	2701	30	1	10.01					
45	UGCA071	J032524.7–161416	1827	9	7	11.27	39	9.63	1.4	0.2	0.54
	MCG...	J032512.1–160950	1816	5	10	13.95					
46	ESO548–025	J032900.7–220848	1715	71	1	11.29	84	9.79	5.3		0.17
	NGC1347	J032941.8–221645	1697	9	5	11.53					
47	IC1970	J033631.5–435725	1085	5	3	9.08	103	10.06	1.0		0.23
	ESO249–008	J033718.9–433510	1094	9	9	12.06					
48	NGC1390	J033752.2–190030	1142	12	6	11.52	171	9.20	0.0		0.57
	ESO548–065	J034002.7–192160	1142	34	8	12.87					
49	NGC1412	J034029.4–265144	1686	12	–2	9.63	35	10.20	4.2		0.24
	ESO482–032	J034041.4–264711	1645	22	7	12.66					
50	NGC1416	J034102.9–224309	2077	24	–5	10.53	133	10.05	59.9		0.03
	2MASX...	J034127.1–222823	2143	75	–4	13.42					
51	NGC1421	J034229.3–132917	2033	9	4	8.37	288	11.02	19.7	19.1	0.34
	MCG...	J034256.1–125459	2111	5	5	9.37					
52	NGC1440	J034502.9–181558	1458	27	–2	8.16	373	10.65	1.0		0.12
	ESO549–007	J034411.5–191910	1448	11	9	12.41					
53	IC0334	J034517.1+763818	2762	7	2	7.62	963	11.41	5.2	3.8	0.58
	HFLZOAG...	J033724.9+751500	2727	9	10	14.11					
54	UGC02906	J040101.0+740502	2837	28	3	8.95	160	10.91	4.6	3.8	0.26
	HFLZOAG...	J040330.7+741503	2793	9	10	14.76					
55	NGC1527	J040824.1–475349	815	38	–3	7.63	351	10.36	2.0		0.21
	AM0358–465	J035956.4–464705	804	9	5	12.12					
56	NGC1533	J040951.8–560706	582	20	–2	7.62	24	10.01	16.8		0.56

Table I: **Table.** (Contd.)

No.	Name	J2000.0	V_{LG}	\pm	T	K	R_\perp	$\log L$	$\frac{M}{L_K}$	$\frac{M^c}{L_K}$	$\log(II)$
			km s $^{-1}$			mag	kpc	L_\odot	\odot	\odot	
	IC2038	J040853.8–555922	505	52	7	14.10					
57	NGC1559	J041735.8–624701	1072	6	6	8.01	249	10.44	0.8		0.24
	ESO084–015	J042211.8–633640	1064	20	9	12.91					
58	IC2059	J042026.3–314328	2653	27	–2	9.89	458	10.57	25.6	15.5	0.72
	ESO420–015	J041741.9–311730	2611	5	10	11.32					
59	ESO550–024	J042113.6–215046	782	6	7	10.06	121	9.36	0.6		0.82
	ESO550–023	J042012.6–211439	785	9	8	14.63					
60	NGC1530	J042327.1+751744	2676	10	3	8.23	874	11.29	1.1	0.1	0.48
	IC0381	J044428.5+753823	2690	5	4	9.30					
61	NGC1638	J044136.5–014833	3235	29	–2	9.20	285	10.95	10.7	9.8	0.22
	UGC03127	J044025.4–020127	3289	5	7	12.62					
62	MCG...	J044834.4–035202	2690	5	–1	10.25	326	10.55	16.7		0.01
	MCG...	J044822.5–032160	2729	35	4	10.86					
63	UGC03180	J045024.2+084247	3384	33	1	10.47	306	10.69	51.7	16.7	2.16
	UGC03188	J045149.2+085038	3467	35	8	10.92					
64	ESO119–016	J045129.2–613903	739	10	10	12.58	74	8.37	13.9		0.08
	SGC...	J045455.4–613353	745	9	10	14.30					
65	2MASX...	J045500.2–371535	2105	74	–1	12.32	34	9.58	44.0		0.62
	ESO361–019	J045453.7–371918	2170	33	7	12.53					
66	2MASX...	J050016.8+711208	1422	38	4	11.98	23	9.13	0.5		0.31
	UGC03212	J050102.2+711033	1418	6	10	14.73					
67	ESO486–021	J050319.7–252523	683	21	3	11.42	14	8.72	8.6		1.01
	ESO486–015	J050300.7–252803	666	75	10	13.72					
68	NGC1784	J050527.1–115218	2192	5	5	8.47	294	10.91	9.3	8.6	0.71
	FGC0523	J050732.0–113906	2239	6	7	11.76					
69	UGCA102	J051048.1–024054	2740	16	3	11.92	51	9.75	15.4		1.91
	IIZw 033B	J051045.3–024531	2778	75	10	14.13					
70	ESO362–009	J051159.3–325821	737	5	8	10.40	57	9.18	11.5	7.0	0.30
	ESO362–007	J051028.3–330109	753	5	10	14.65					
71	NGC1924	J052801.9–051839	2423	5	4	9.30	485	10.66	0.2		1.81
	MCG...	J052709.2–060705	2427	74	10	12.36					
72	ESO487–020	J053223.8–251355	1750	74	7	13.19	130	8.93	779.5		0.35
	AM0530–245	J053246.5–245533	1684	74	10	14.16					
73	NGC1954	J053248.3–140346	2973	5	4	9.05	116	11.19	48.5	47.8	0.29
	IC2132	J053228.7–135538	3205	18	1	9.37					
74	MCG...	J053653.2–151215	3087	9	0	9.87	122	10.65	25.0	23.2	0.29
	2MASX...	J053612.6–151438	2999	12	5	12.33					
75	ESO554–027	J054306.1–203117	2839	33	–1	11.38	103	10.13	111.5		1.03

Table I: **Table.** (Contd.)

No.	Name	J2000.0	V_{LG}	\pm	T	K	R_\perp	$\log L$	$\frac{M}{L_K}$	$\frac{M^c}{L_K}$	$\log(II)$
			km s $^{-1}$			mag	kpc	L_\odot	\odot	\odot	
	2MASX...	J054305.9–204014	2950	74	0	12.14					
76	NGC2076	J054646.7–164708	1982	8	-1	8.94	313	10.60	2.4		0.57
	HIPASS...	J054423.6–162652	1966	25	8	13.72					
77	NGC2104	J054704.7–513311	914	10	9	10.56	121	9.34	50.6	38.4	1.13
	NGC2101	J054624.2–520519	942	6	10	13.01					
78	NGC2106	J055046.6–213402	1724	6	-2	9.11	407	10.42	10.5	4.7	0.83
	ESO555–010	J055257.5–204246	1700	9	9	12.91					
79	IC0438	J055300.1–175234	2939	6	5	9.68	91	10.76	0.2		0.05
	IC2151	J055236.4–174714	2930	10	4	11.04					
80	IC2153	J060004.2–335512	2617	15	5	11.25	3	10.15	0.1		0.61
	IC2153...	J060005.4–335505	2599	28	5	11.60					
81	IC0441	J060242.6–122957	2047	5	5	10.74	232	10.20	2.2	0.4	1.68
	MCG...	J060434.9–123729	2058	5	3	10.82					
82	ESO425–014	J061302.7–274347	2718	28	-3	9.38	595	10.75	32.1		1.05
	ESO425–010	J060857.3–274812	2769	56	8	11.92					
83	NGC2211	J061830.4–183214	1784	20	-2	9.36	12	10.39	0.7	0.3	0.15
	NGC2212	J061835.8–183110	1818	11	6	12.06					
84	NGC2221	J062015.7–573442	2262	50	3	10.05	26	10.40	6.1	2.8	0.49
	NGC2222	J062016.1–573151	2332	11	4	11.39					
85	UGC03445	J062132.8+590736	3241	22	2	8.60	10	11.35	0.1		0.82
	UGC03446	J062138.9+590733	3291	35	1	9.38					
86	NGC2223	J062435.9–225018	2502	19	4	8.83	128	10.90	60.2	19.6	0.27
	ESO489–052	J062520.6–224327	2679	74	4	12.45					
87	PGC179437	J062501.7–372252	2607	8	-1	12.39	19	9.75	0.3		1.47
	2MASX...	J062456.0–372126	2616	74	3	12.45					
88	6dF...	J062534.5–282716	2597	74	-1	10.90	193	10.30	101.9		1.11
	ESO426–010	J062639.3–283952	2503	6	3	11.12					
89	ESO122–001	J064043.2–583128	2376	30	3	9.26	32	10.68	6.0	4.8	1.47
	ESO122–002	J064046.6–582811	2463	18	5	12.09					
90	NGC2273	J065008.7+605045	1968	10	1	8.45	382	10.78	17.8		0.49
	MAILYAN017	J064639.2+600845	1919	75	10	14.02					
91	UGC03509	J065455.4+853817	1865	46	2	11.20	77	9.65	77.8	70.9	0.44
	UGC03496	J065036.0+854742	1804	5	10	15.04					
92	UGC03647	J070450.4+563113	1488	5	10	12.12	44	9.28	0.7		0.95
	CGCG...	J070359.2+562911	1493	25	10	12.73					
93	UGC03657	J070724.1+711133	3427	75	6	13.50	153	9.49	19.6		0.17
	UGC03644	J070538.2+710413	3409	11	7	13.87					
94	NGC2337	J071013.6+442726	477	5	8	10.31	20	8.82	5.3	1.6	0.83

Table I: **Table.** (Contd.)

No.	Name	J2000.0	V_{LG} km s $^{-1}$	\pm	T	K mag	R_\perp kpc	$\log L$ L_\odot	$\frac{M}{L_K}$ \odot	$\frac{M^c}{L_K}$ \odot	$\log(II)$
	UGC03698	J070918.7+442248	465	5	10	14.24					
95	UGC03730...	J071420.6+732850	2897	18	2	10.78	106	10.41	6.6	2.6	0.89
	UGC03705	J071211.2+732814	2860	11	9	11.27					
96	NGC2268	J071417.4+842256	2440	5	4	8.56	391	10.94	41.4	40.8	0.26
	UGC03522	J065606.1+845504	2352	5	10	12.12					
97	NGC2357	J071741.0+232124	2204	5	6	9.61	484	10.59	11.5	10.1	0.40
	UGC03751	J071353.9+230449	2232	5	6	10.51					
98	UGC03788	J071825.9+313340	3443	7	4	11.15	142	10.29	0.5		0.68
	UGC03790...	J071833.0+312327	3451	56	7	12.73					
99	UGC03789	J071930.9+592118	3396	58	2	9.49	60	10.88	13.6	12.5	0.18
	UGC03797	J072003.1+592243	3517	15	6	13.40					
100	NGC2276	J072714.4+854516	2632	12	5	9.68	111	10.70	31.3	27.4	0.53
	UGC03654	J071747.1+854248	2523	22	-3	10.48					
101	IC2202	J072754.7-673427	3327	6	4	9.40	566	10.96	0.0		0.21
	ESO058-028	J072034.0-674239	3324	10	7	10.97					
102	UGC03864	J073057.0+723102	2737	50	5	12.40	5	9.51	1.0		0.55
	VV141b	J073054.8+723037	2714	75	10	15.83					
103	UGC03974	J074155.4+164809	162	5	10	11.40	11	7.54	11.7		1.69
	CGCG...	J074232.0+163340	168	5	10	13.11					
104	ESO035-018	J075504.2-762445	1492	5	5	9.76	288	10.04	4.6		0.73
	ESO035-020	J080318.6-770419	1479	9	9	13.15					
105	UGC04159	J080151.2+612447	1703	8	9	11.50	37	9.60	0.0		0.50
	UGC04169	J080234.1+612253	1701	5	9	12.42					
106	UGC04151	J080418.7+774860	2473	5	6	10.39	276	10.30	3.2	1.6	0.70
	UGC04066	J075615.6+780048	2487	5	8	12.09					
107	ESO124-014	J080912.7-613937	2708	20	-3	9.29	231	10.93	7.7		1.54
	IRAS...	J080852.5-611835	2756	44	3	10.00					
108	LCSBS1123P	J081715.9+245357	1832	5	9	13.68	29	8.75	41.0		0.88
	KUG0814...	J081721.0+245746	1806	70	9	14.99					
109	CGCG...	J081725.4+210950	2054	9	8	13.12	10	9.24	5.9		0.46
	CGCG...	J081728.1+211052	2024	75	4	13.20					
110	IC2267	J081801.5+244411	1962	10	6	11.84	29	9.57	11.2	9.4	0.75
	IC2268	J081806.6+244747	1928	5	9	12.90					
111	NGC2549	J081858.3+574811	1154	22	-2	8.02	127	10.51	0.5		0.50
	UGC04314	J081857.8+581547	1164	7	9	12.24					
112	6dF...	J082142.8-002601	1612	74	10	12.88	27	8.97	1.2		1.93
	UGC04358	J082126.0-002508	1606	6	10	14.03					
113	SAO0822+3545	J082605.6+353526	671	50	10	15.02	10	7.48	133.2		1.57

Table I: **Table.** (Contd.)

No.	Name	J2000.0	V_{LG} km s $^{-1}$	\pm	T	K mag	R_\perp kpc	$\log L$ L_\odot	$\frac{M}{L_K}$ \odot	$\frac{M^c}{L_K}$ \odot	$\log(II)$
	SDSS...	J082555.5+353232	690	18	9	15.37					
114	UGC04393	J082604.4+455804	2156	12	6	11.21	116	9.83	10.8	7.6	0.61
	MCG...	J082718.1+460200	2179	5	9	13.37					
115	NGC2607	J083356.6+265821	3452	9	6	12.02	137	9.89	55.9		0.90
	SDSS...	J083326.0+265114	3503	37	8	15.03					
116	NGC2619	J083732.7+284219	3408	5	3	9.59	573	10.93	0.3		0.90
	KUG0833...	J083615.4+280337	3401	5	5	10.86					
117	NGC2644	J084131.9+045849	1780	32	5	10.35	309	9.96	3.5		1.05
	UGC04524	J084014.4+053804	1771	7	7	14.25					
118	UGC04543	J084321.6+454408	1983	5	8	12.43	42	9.24	3.3		1.27
	NPM1G...	J084253.9+454632	1972	75	9	15.32					
119	UGC04559	J084407.6+300709	2024	6	3	10.01	284	10.19	0.0		0.66
	SDSS...	J084442.7+293243	2025	8	9	15.57					
120	UGC04587	J084722.7+493331	3089	45	2	10.14	317	10.52	20.5		0.37
	SDSS...	J084955.0+494013	3132	21	8	14.61					
121	UGC04621	J085011.8+350436	2264	8	2	10.41	119	10.15	28.1		0.17
	KUG0847...	J085052.9+345435	2317	41	9	14.85					
122	UGCA147	J085107.1-173349	1732	5	6	10.16	140	10.02	51.0		0.48
	2MASX...	J085152.7-175116	1675	74	7	12.84					
123	NGC2683	J085241.4+332519	366	5	3	6.32	35	10.25	6.9	6.7	0.53
	[KK98]069	J085250.8+334752	420	5	10	14.31					
124	NGC2684	J085454.0+490937	2918	18	6	10.37	303	10.48	0.5		0.59
	SBS0849+496	J085258.4+492738	2924	8	9	11.70					
125	NGC2685	J085534.7+584404	966	7	-1	8.33	109	10.25	20.2	19.4	1.14
	UGC04683	J085754.4+590458	1018	5	10	13.95					
126	2MASX...	J085828.2-184717	3260	74	-1	10.81	157	10.28	155.6		1.10
	ESO564-003	J085902.9-183806	3134	97	8	14.97					
127	UGC04703...	J085829.8+061917	3373	7	9	13.10	20	9.47	3.0		0.23
	UGC04703...	J085825.0+062006	3353	23	10	14.97					
128	NGC2721	J085856.5-045407	3483	6	4	9.71	63	10.77	17.0	16.0	0.51
	FGC0821	J085914.4-045249	3367	14	8	14.84					
129	NGC2701	J085905.7+534618	2392	5	5	9.67	317	10.48	23.1	21.8	0.95
	SDSS...	J085618.6+540818	2435	5	8	15.08					
130	UGC04730	J090158.4+600906	3377	63	0	10.37	25	10.49	1.8		1.65
	UGC04727	J090143.9+600927	3333	75	6	15.09					
131	ESO564-011	J090246.2-204331	2498	9	0	10.46	7	10.30	4.3		0.50
	ESO564-010	J090244.9-204251	2598	74	10	12.12					
132	IC0512	J090349.8+853006	1830	11	6	9.90	33	10.15	0.3		0.05

Table I: **Table.** (Contd.)

No.	Name	J2000.0	V_{LG} km s $^{-1}$	\pm	T	K mag	R_\perp kpc	$\log L$ L_\odot	$\frac{M}{L_K}$ \odot	$\frac{M^c}{L_K}$ \odot	$\log(II)$
	UGC04612	J090018.6+853156	1820	11	9	14.33					
133	KUG0901...	J090440.1+472415	2310	35	4	13.34	123	9.16	340.3		1.80
	SDSS...	J090331.1+473028	2368	67	9	14.15					
134	ESO564-019	J090527.5-183130	1730	74	4	11.30	211	9.81	90.6		0.48
	NGC2758	J090531.2-190234	1682	5	4	11.40					
135	NGC2772	J090741.9-233717	3139	5	3	9.33	7	10.86	0.5	0.4	0.91
	ESO-LV...	J090741.1-233749	3205	15	10	15.28					
136	NGC2764	J090817.5+212636	2608	5	-2	9.80	104	10.50	1.1	0.7	0.88
	LSBC...	J090855.3+212149	2591	5	9	14.39					
137	UGC04809	J090920.3+204150	2907	8	6	11.97	91	9.82	18.3	13.3	0.91
	MCG...	J090904.6+203452	2873	9	9	13.40					
138	CGCG...	J091023.5+192719	3007	10	-1	11.43	44	10.02	0.0		0.80
	UGC04822	J091038.5+192823	3005	5	8	13.72					
139	UGCA150	J091048.8-085338	1591	5	3	7.69	157	10.92	0.2		0.10
	2MASX...	J090939.9-083547	1600	74	9	13.41					
140	NGC2784	J091219.5-241021	407	35	-2	6.24	132	10.34	7.0	3.4	0.21
	ESO497-017	J090946.5-230033	438	11	10	11.81					
141	IC2445	J091312.6+314828	1859	9	6	12.78	65	9.08	14.2	5.4	0.58
	SDSS...	J091251.7+314051	1844	5	8	14.70					
142	KUG0910...	J091340.9+331930	3374	42	5	13.16	128	9.63	0.0		0.85
	UGC04850	J091304.6+332517	3375	20	8	13.43					
143	NGC2785	J091515.4+405503	2728	10	7	9.41	81	10.69	6.5	6.2	0.21
	SDSS...	J091435.6+405524	2671	6	7	14.58					
144	ESO497-029	J091543.3-234205	3134	14	6	11.76	113	10.03	0.0		0.91
	ESO497-028	J091534.4-235053	3134	74	9	12.65					
145	NGC2811	J091611.1-161846	2099	29	1	7.96	165	11.02	44.9	4.5	0.61
	6dF...	J091648.3-160022	1944	74	9	12.74					
146	NGC2815	J091619.8-233760	2258	8	3	8.20	125	11.03	7.1	4.9	0.04
	NGC2815:...	J091547.6-232628	2330	20	9	14.93					
147	IC0529	J091832.8+734534	2422	5	5	9.47	275	10.62	3.9		0.43
	CGCG...	J091215.0+733539	2445	18	9	11.65					
148	NGC2787	J091918.6+691212	838	5	-1	7.21	187	10.51	41.0	39.8	0.28
	UGC04998	J092511.0+682259	761	7	10	13.16					
149	NGC2858	J092255.0+030925	3446	32	0	9.80	93	10.76	0.4		0.21
	2MASX...	J092234.1+030501	3432	36	-1	12.91					
150	NGC2852	J092314.6+400950	1778	25	1	10.09	16	10.16	0.5		0.39
	NGC2853	J092317.3+401200	1758	30	4	11.41					
151	UGC04984	J092339.7+542900	3452	63	9	13.50	165	9.36	318.8		1.61

Table I: **Table.** (Contd.)

No.	Name	J2000.0	V_{LG} km s $^{-1}$	\pm	T	K mag	R_\perp kpc	$\log L$ L_\odot	$\frac{M}{L_K}$ \odot	$\frac{M^c}{L_K}$ \odot	$\log(II)$
	SBS0919+545	J092316.4+541734	3513	18	9	15.11					
152	ESO498–003	J092336.5–265255	2070	10	3	9.73	54	10.35	6.6		0.35
	ESO497–042	J092312.0–265627	2118	75	5	13.39					
153	NGC2891	J092656.6–244659	2067	20	-3	9.52	300	10.61	25.9	6.9	0.46
	ESO498–005	J092440.7–250534	2121	25	4	10.17					
154	UGC05052	J093114.0+734838	3253	19	2	10.28	313	10.68	66.9		0.64
	CGCG...	J092540.4+735400	3346	66	3	11.11					
155	MCG...	J093612.4–082604	1701	59	-4	9.76	175	10.17	6.3		0.74
	MCG...	J093520.4–084836	1680	6	9	12.46					
156	NGC2979	J094308.7–102260	2451	31	1	9.50	257	10.70	0.0		0.98
	MCG...	J094317.9–095644	2449	5	7	10.62					
157	NGC2983	J094341.1–202838	1767	45	-1	8.52	94	10.66	5.9		0.41
	6dF...	J094356.9–204142	1717	74	8	13.05					
158	NGC3020	J095006.6+124849	1283	5	6	10.67	30	9.74	3.6	3.0	1.23
	NGC3024	J095027.4+124556	1260	5	7	11.17					
159	UGC05272	J095022.4+312916	460	5	10	12.01	4	8.14	2.8		0.86
	UGC05272b	J095019.4+312721	469	13	10	15.32					
160	NGC3032	J095208.2+291410	1472	12	-2	9.64	70	10.09	54.0	52.6	0.46
	KUG0950...	J095257.6+291837	1561	7	8	15.77					
161	NGC3052	J095427.9–183820	3502	5	5	9.41	650	11.09	36.6	35.7	0.10
	ESO566–019	J095113.4–182833	3425	7	6	10.04					
162	NGC3044	J095340.9+013447	1115	34	6	8.97	29	10.11	7.4	3.2	0.72
	APMUKS...	J095404.6+013224	1168	20	10	17.94					
163	NGC3055	J095518.1+041612	1626	18	5	9.48	82	10.22	0.2		0.24
	SDSS...	J095435.7+042308	1620	66	9	14.81					
164	NGC3043	J095614.8+591826	3082	15	5	10.45	256	10.40	0.1		0.45
	SBS0953+592	J095722.4+585929	3085	5	9	14.46					
165	NGC3065	J100155.3+721013	2160	10	0	8.97	26	10.83	2.0	0.9	0.45
	NGC3066	J100211.1+720731	2227	29	4	9.92					
166	UGC05403	J100235.5+191037	1958	10	1	10.32	67	10.03	47.9	47.1	1.58
	UGC05401	J100231.2+190158	1877	5	9	14.52					
167	NGC3107	J100422.5+133717	2652	7	4	10.32	477	10.44	0.1		0.15
	CGCG...	J100551.2+125741	2653	5	1	11.40					
168	NGC3124	J100639.9–191318	3285	5	4	9.07	152	10.99	13.6	7.0	0.13
	2MASX...	J100711.1–190405	3199	30	4	13.49					
169	NGC3118	J100711.6+330140	1291	5	4	11.66	51	9.25	56.1		0.71
	UGC05446	J100630.9+325647	1332	42	6	13.19					
170	ESO567–018	J100726.2–212836	3307	30	3	10.86	346	10.39	28.7		0.50

Table I: **Table.** (Contd.)

No.	Name	J2000.0	V_{LG}	\pm	T	K	R_\perp	$\log L$	$\frac{M}{L_K}$	$\frac{M^c}{L_K}$	$\log(II)$
			km s $^{-1}$			mag	kpc	L_\odot	\odot	\odot	
	ESO567–014	J100548.5–211547	3349	74	7	12.28					
171	IC0591	J100727.7+121628	2659	12	4	11.25	242	10.08	15.1	9.5	0.40
	UGC05454	J100711.0+123905	2634	5	9	12.18					
172	CGCG...	J100757.1+131339	2605	11	6	12.34	96	9.54	12.5	7.5	0.07
	SDSS...	J100733.2+130624	2585	5	9	14.28					
173	MCG...	J100903.3–111360	3216	33	–2	9.78	37	10.80	42.7	29.2	0.03
	2MASX...	J100906.5–111119	3462	74	0	11.61					
174	IC0598	J101248.6+430844	2263	13	2	10.14	168	10.24	20.2		1.25
	KUG1008...	J101152.9+432432	2222	31	9	14.62					
175	NGC3153	J101250.5+124000	2656	5	6	10.60	354	10.20	10.2		0.65
	SDSS...	J101033.9+123540	2636	11	8	14.98					
176	IC2558	J101444.1–342019	2292	35	7	11.09	180	9.91	3.1		0.05
	ESO375–003	J101553.8–340653	2303	9	9	13.68					
177	ESO500–018	J101453.7–230302	3409	27	–2	9.64	358	10.79	73.9		0.25
	2MASX...	J101426.8–232904	3305	74	4	13.80					
178	UGC05541	J101655.4+582342	2344	5	10	13.52	84	9.00	46.2	36.3	0.49
	SDSS...	J101712.2+583225	2366	5	9	15.21					
179	IC0600	J101710.9–032952	1082	5	8	11.70	4	8.97	31.4	25.9	1.37
	LCRS...	J101712.7–032901	1003	17	10	14.58					
180	NGC3184	J101817.0+412528	589	5	6	7.22	394	10.25	1.1		0.09
	NGC3104	J100357.4+404525	595	7	10	11.19					
181	ESO567–052	J102008.0–214143	3251	27	–2	10.83	21	10.47	3.5		0.29
	ESO567–053	J102008.9–214319	3187	59	4	11.43					
182	NGC3206	J102147.6+565550	1239	5	6	11.15	85	9.54	16.1		0.38
	NGC3220	J102344.7+570137	1262	16	6	11.59					
183	UGC05646	J102553.1+142147	1223	5	5	10.94	145	9.49	13.7	8.2	1.01
	UGC05633	J102440.1+144526	1239	5	8	12.42					
184	NGC3246	J102641.8+035143	1957	23	8	10.72	301	9.90	1.5		1.44
	VIIIIZw 081	J102848.1+041405	1951	5	9	14.15					
185	UGC05707	J103114.3+430815	2807	5	6	14.03	32	9.05	55.8	52.5	2.14
	SDSS...	J103118.6+430534	2848	5	9	14.80					
186	IC2594	J103604.2–241923	3265	20	–3	9.32	120	11.03	0.1		0.08
	ESO501–024	J103527.2–242303	3274	28	–1	10.37					
187	NGC3294	J103616.3+371929	1556	14	5	8.38	150	10.66	49.8	30.8	0.73
	KUG1032...	J103522.8+374018	1669	35	9	12.91					
188	NGC3301	J103656.0+215256	1240	17	–1	8.51	160	10.47	10.9	8.7	0.22
	NGC3287	J103447.3+213854	1199	5	8	9.77					
189	NGC3306	J103710.2+123909	2738	5	8	10.40	325	10.33	18.7	15.3	0.47

Table I: **Table.** (Contd.)

No.	Name	J2000.0	V_{LG} km s $^{-1}$	\pm	T	K mag	R_\perp kpc	$\log L$ L_\odot	$\frac{M}{L_K}$ \odot	$\frac{M^c}{L_K}$ \odot	$\log(II)$
	CGCG...	J103723.4+120924	2706	7	8	13.01					
190	IC0630	J103833.8-071015	1930	10	9	8.63	85	10.70	30.9		0.40
	MRK1258	J103800.4-071802	1806	75	9	11.84					
191	NGC3320	J103936.5+472353	2353	7	4	10.09	356	10.30	10.8		0.78
	SDSS...	J104309.7+471258	2375	19	7	15.00					
192	6dF...	J104011.8-095640	2218	74	6	13.43	128	9.07	221.4		0.90
	6dF...	J103930.4-094609	2177	74	9	14.18					
193	AM1039-313...	J104120.7-314855	2388	74	0	10.58	24	10.25	8.1		0.50
	ESO437-042	J104127.7-314649	2317	18	5	11.49					
194	ESO568-021	J104115.2-210123	3322	75	3	11.15	385	10.26	73.0		0.60
	ESO568-023	J104248.5-204147	3268	14	7	12.67					
195	ESO569-001	J104409.1-204809	3375	37	-2	11.02	14	10.28	16.0		0.19
	2MASX...	J104409.7-204910	3511	74	5	13.80					
196	NGC3329	J104439.4+764834	2113	27	3	9.40	60	10.49	27.3		1.12
	UGC05841	J104456.0+764117	2004	83	5	11.93					
197	NGC3348	J104710.0+725023	2993	27	-5	7.94	299	11.40	20.2	11.4	0.04
	NGC3364	J104829.8+722530	2874	41	5	10.10					
198	UGC05897	J104741.5+110437	2575	16	5	10.25	116	10.42	22.5	21.0	0.42
	CGCG...	J104753.9+105352	2640	5	6	11.72					
199	NGC3398	J105131.4+552328	2943	75	3	10.76	388	10.25	100.8		0.77
	MCG...	J104835.3+554442	3006	37	9	14.02					
200	NGC3434	J105158.0+034731	3445	9	3	9.74	37	10.77	1.4	1.3	0.09
	CGCG...	J105200.2+035010	3402	5	8	13.61					
201	NGC3432	J105231.1+363708	589	5	9	9.06	158	9.52	3.1		0.70
	CGCG...	J105747.0+361539	596	17	10	13.32					
202	CGCG...	J105248.6+000204	1607	5	9	12.97	25	8.82	65.3		0.91
	MGC0013223	J105240.6-000117	1569	75	10	16.40					
203	LSBC...	J105318.6+023734	851	10	9	13.45	30	8.17	18.9		0.50
	LSBC...	J105303.1+022937	860	5	10	14.89					
204	NGC3448	J105439.2+541819	1448	27	3	9.47	24	10.16	26.5	25.7	0.95
	UGC06016	J105412.8+541714	1564	10	10	14.60					
205	ESO376-027	J105658.2-330952	3436	53	5	11.84	4	10.08	6.1	3.0	0.97
	ESO-LV...	J105659.1-330939	3560	40	7	12.92					
206	ESO569-030	J105824.2-190912	3257	30	4	13.06	62	9.57	64.5		0.08
	2MASX...	J105844.2-190931	3314	74	4	13.82					
207	UGC06074	J105958.3+505411	2946	5	9	10.57	41	10.31	0.1		1.41
	MCG...	J110006.4+505056	2952	5	8	14.03					
208	BTS029	J110138.9+303629	1626	5	10	14.08	12	8.61	240.3		0.80

Table I: **Table.** (Contd.)

No.	Name	J2000.0	V_{LG}	\pm	T	K	R_\perp	$\log L$	$\frac{M}{L_K}$	$\frac{M^c}{L_K}$	$\log(II)$
			km s $^{-1}$			mag	kpc	L_\odot	\odot	\odot	
	BTS028	J110132.4+303516	1708	75	9	14.58					
209	NGC3504	J110311.2+275821	1467	8	2	8.26	67	10.67	42.7	42.4	0.15
	NGC3512	J110403.0+280213	1307	7	5	9.64					
210	NGC3547	J110955.9+104315	1428	5	3	10.43	59	9.76	20.2		0.36
	CGCG...	J110923.3+105003	1387	75	9	12.64					
211	NGC3543	J111056.4+612049	1779	5	4	11.40	200	9.56	1.2		0.57
	[HS98]137A	J110718.0+613127	1783	5	10	14.20					
212	NGC3549	J111056.9+532316	2932	5	5	9.18	370	10.86	0.0		0.64
	CGCG...	J111350.5+530511	2934	40	7	13.13					
213	NGC3544	J111130.5–181722	3465	20	1	8.97	66	11.07	5.1	2.7	0.24
	NGC3571:...	J111119.6–181315	3378	30	8	14.15					
214	ESO377–019	J111045.4–352102	2699	11	7	11.11	327	10.23	121.8		0.13
	2MASX...	J111252.5–353614	2772	74	6	11.58					
215	CGCG...	J111540.4+460739	2901	5	9	13.31	23	9.25	17.7	16.1	0.75
	SDSS...	J111550.5+460638	2934	5	9	15.41					
216	UGC06309	J111746.5+512836	2931	6	4	10.57	40	10.30	12.3	12.0	0.39
	MRK1445	J111732.3+512553	2860	5	9	14.23					
217	NGC3617	J111750.9–260804	1886	8	-4	9.76	43	10.25	38.4	38.1	0.78
	ESO503–011	J111744.4–260223	1770	5	6	12.08					
218	NGC3621	J111816.5–324851	437	5	7	6.57	317	10.21	18.2	10.8	0.80
	HIPASS...	J113311.1–325745	409	9	9	13.65					
219	NGC3614	J111821.3+454454	2366	14	5	9.63	34	10.47	4.5		0.36
	SDSS...	J111826.7+454124	2308	35	9	15.47					
220	UGC06355	J112039.8+311320	2142	5	6	12.52	23	9.38	13.8		1.46
	2MASX...	J112046.0+311059	2107	30	9	13.44					
221	NGC3631	J112102.9+531011	1227	7	5	7.98	150	10.64	12.9	11.7	0.13
	NGC3657	J112355.6+525515	1283	9	-1	10.28					
222	UGC06402	J112319.1–005521	2412	5	8	11.21	80	9.89	14.7	4.2	1.70
	SDSS...	J112344.8–005011	2446	15	10	14.49					
223	NGC3687	J112800.6+293039	2453	12	4	10.23	7	10.23	40.5	39.9	1.46
	2MASX...	J112804.2+293038	2168	18	9	14.38					
224	NGC3694	J112854.1+352450	2254	27	1	10.39	280	10.14	60.8	57.0	0.86
	UGC06499	J113011.3+355208	2204	5	10	14.56					
225	NGC3705	J113007.5+091636	868	5	2	7.90	190	10.31	2.6		0.14
	IC2828	J112710.9+084352	883	12	9	12.64					
226	SBS1129+576	J113202.5+572246	1660	5	8	14.48	23	8.44	19.9		0.09
	SDSS...	J113227.7+572142	1646	33	9	15.02					
227	IC0705	J113256.3+501430	3005	42	-1	11.41	175	10.01	65.6	37.7	0.00

Table I: **Table.** (Contd.)

No.	Name	J2000.0	V_{LG}	\pm	T	K	R_\perp	$\log L$	$\frac{M}{L_K}$	$\frac{M^c}{L_K}$	$\log(II)$
			km s $^{-1}$			mag	kpc	L_\odot	\odot	\odot	
	SDSS...	J113342.5+502659	3062	16	9	14.39					
228	UGC06535	J113313.4+501808	3209	16	6	12.20	116	9.72	101.0		0.00
	SDSS...	J113253.4+500933	3147	46	9	16.09					
229	UGC06538	J113316.9+491705	3131	49	10	13.59	44	9.25	52.5		0.38
	SDSS...	J113319.8+492036	3173	18	8	14.95					
230	SDSS...	J113342.7+482005	3094	20	9	15.41	114	8.64	51.1		0.78
	SDSS...	J113403.9+482837	3107	29	9	15.77					
231	NGC3731	J113411.7+123044	3079	19	-5	10.27	300	10.46	3.1		0.76
	IC2929	J113331.5+120814	3063	11	4	14.20					
232	UGC06570	J113550.0+352007	1580	10	1	10.72	179	9.75	51.4	46.5	0.20
	UGC06603	J113802.1+351213	1617	5	6	13.01					
233	NGC3755	J113633.4+362437	1557	5	5	10.59	28	9.75	4.0		0.20
	HS1134+3639	J113654.7+362316	1583	36	9	14.88					
234	NGC3756	J113648.0+541737	1369	5	4	8.77	323	10.38	22.5		0.37
	SBS1139+550	J114227.2+544908	1406	50	0	12.06					
235	MRK0745	J113956.3+165718	3100	9	2	12.22	27	9.93	0.7		0.23
	CGCG...	J113949.6+165849	3086	7	8	12.51					
236	ESO266-015	J114055.7-442853	2886	5	4	9.70	68	10.65	0.1		0.20
	6dF...	J114059.2-442302	2894	74	4	12.77					
237	KUG1138...	J114107.4+322537	1704	70	10	14.13	45	8.68	45.0		0.75
	MRK0746	J114129.9+322059	1684	50	9	14.17					
238	NGC3818	J114157.4-060920	1493	7	-5	8.85	128	10.43	3.6	2.4	0.58
	UGCA242	J114122.5-062853	1518	8	9	11.52					
239	ESO571-016	J114209.1-181008	3385	7	4	10.42	112	10.51	28.5		0.81
	6dF...	J114135.0-181141	3469	74	10	13.38					
240	ESO572-001	J114638.5-204435	3330	74	4	12.53	256	9.82	204.8		1.81
	2MASX...	J114515.2-204447	3263	74	5	13.07					
241	NGC3892	J114801.0-105743	1519	59	-1	8.34	384	10.64	11.0		0.30
	UGCA245	J114526.2-100610	1487	5	6	11.09					
242	2MASX...	J115009.4-040232	1480	74	-1	12.15	155	9.16	663.4		0.15
	LCRS...	J114912.8-033934	1408	12	6	13.49					
243	UM456	J115036.2-003402	1574	5	8	12.75	12	9.07	59.8	50.8	0.92
	UM456A	J115034.0-003216	1645	16	8	13.55					
244	UGC06814	J115038.1+642101	3147	24	5	13.42	37	9.33	2.2		1.35
	SDSS...	J115102.2+641938	3157	39	9	14.65					
245	UGC06850	J115237.4-022810	862	12	9	12.97	58	8.39	26.3		0.72
	UM461	J115133.4-022222	852	5	9	14.17					
246	NGC3936	J115220.6-265421	1756	6	4	9.04	281	10.50	0.4		0.12

Table I: **Table.** (Contd.)

No.	Name	J2000.0	V_{LG} km s $^{-1}$	\pm	T	K mag	R_\perp kpc	$\log L$ L_\odot	$\frac{M}{L_K}$ \odot	$\frac{M^c}{L_K}$ \odot	$\log(II)$
	ESO504–028	J115454.4–271505	1762	5	7	11.41					
247	NGC3952	J115340.6–035948	1382	5	9	11.00	103	9.74	2.5		0.35
	IC2969	J115231.3–035220	1372	6	4	11.14					
248	KDG083	J115614.5+311816	617	5	–3	11.31	125	8.72	165.0		0.43
	KUG1157...	J120016.2+311330	593	28	4	12.87					
249	UGC06927	J115708.5+302332	3334	32	–2	10.61	443	10.43	38.7	24.0	0.46
	IC2985	J115912.7+304352	3290	10	7	13.06					
250	IC2986	J115949.6+305040	3107	21	–2	11.17	195	10.14	27.8		0.21
	CGCG...	J120103.7+305039	3066	40	5	13.49					
251	IC0755	J120110.4+140616	1396	8	3	11.32	33	9.47	11.4	8.5	0.25
	MRK0756	J120127.5+140204	1366	8	4	12.39					
252	KUG1159...	J120225.1+292812	3336	32	7	12.96	113	9.48	40.7		0.73
	KISSLB083	J120303.7+292653	3366	75	9	16.03					
253	SBS1203+592	J120614.2+585816	3367	7	9	13.78	62	9.23	0.2		0.39
	SDSS...	J120544.3+590047	3365	62	8	15.16					
254	NGC4112	J120709.5–401229	2400	45	3	9.17	23	10.69	2.9		0.02
	ESO321–007	J120722.1–401304	2329	74	5	12.49					
255	NGC4119	J120809.6+102244	1525	26	–1	8.48	343	10.55	9.3	8.1	0.30
	SDSS...	J121201.2+102354	1496	5	8	15.08					
256	NGC4127	J120826.4+764815	2004	5	5	10.01	333	10.21	33.0	20.8	0.36
	UGC07265	J121504.9+761408	2041	11	8	13.79					
257	ESO441–012	J120927.2–323055	1913	10	2	10.17	262	10.15	40.4	36.5	0.00
	ESO441–007	J120815.6–320031	1956	6	4	12.30					
258	NGC4141	J120947.3+585057	2079	57	6	11.36	59	9.70	5.4		1.10
	SDSS...	J120858.7+584732	2060	16	8	14.59					
259	ESO321–010	J121142.1–383255	2861	6	4	10.34	410	10.39	7.7		0.12
	6dF...	J121143.0–390845	2881	74	9	13.59					
260	NGC4162	J121152.5+240725	2512	5	4	9.35	69	10.64	5.4		0.07
	KUG1209...	J121134.9+240144	2458	75	10	14.63					
261	NGC4165	J121211.8+131448	1764	17	2	10.48	120	9.91	28.5	26.1	0.29
	SDSS...	J121317.8+130936	1804	5	8	14.08					
262	NGC4194	J121409.5+543137	2603	18	9	9.62	382	10.58	10.3	9.1	0.45
	SDSS...	J121250.4+550625	2633	5	9	15.38					
263	UGC07249	J121436.9+124843	509	5	8	12.73	13	7.96	11.6		0.27
	SDSS...	J121412.1+124658	501	11	8	14.89					
264	NGC4203	J121505.1+331150	1078	5	–3	7.40	483	10.71	24.5	23.4	0.13
	UGC07428	J122202.5+320543	1125	5	10	12.83					
265	ESO321–016	J121526.7–380839	2901	8	6	10.89	72	10.20	1.3	0.7	0.12

Table I: **Table.** (Contd.)

No.	Name	J2000.0	V_{LG} km s $^{-1}$	\pm	T	K mag	R_\perp kpc	$\log L$ L_\odot	$\frac{M}{L_K}$ \odot	$\frac{M^c}{L_K}$ \odot	$\log(II)$
	ESO321–018	J121554.3–380536	2885	5	10	13.30					
266	NGC4217	J121550.9+470530	1085	5	3	7.58	199	10.80	18.0	6.4	0.20
	NGC4220	J121611.7+475260	1015	35	0	8.13					
267	UGC07298	J121630.1+521339	254	5	10	12.55	12	7.44	44.8		0.70
	CGCG...	J121546.8+522317	245	15	10	14.25					
268	NGC4238	J121655.8+632436	2908	11	7	11.03	52	10.11	2.4	0.1	0.64
	SDSS...	J121617.2+632318	2930	11	9	15.46					
269	ESO380–008	J121658.2–372816	1835	5	8	11.40	79	9.59	1.4		1.16
	ESO380–009	J121731.9–371946	1828	9	10	14.06					
270	NGC4290	J122047.5+580533	3143	9	3	9.29	610	10.88	0.6		0.37
	MCG...	J122634.9+574951	3151	67	6	13.22					
271	KUG1218...	J122054.9+382549	623	46	9	12.97	68	8.02	1287.8	395.8	0.29
	KDG105	J122143.0+375914	582	5	10	15.07					
272	VCC0513	J122157.8+022042	1699	5	2	12.07	191	9.43	0.3		0.06
	VCC0597	J122256.6+024449	1697	16	3	12.56					
273	NGC4369	J122436.2+392259	1053	29	1	8.91	154	10.09	29.7	28.0	0.03
	PGC166134	J122207.0+394442	1098	5	10	14.66					
274	SBS1222+614	J122505.4+610911	832	5	9	13.03	18	8.48	0.1		0.86
	MCG...	J122453.8+610349	833	5	10	13.20					
275	NGC4384	J122512.0+543022	2616	11	1	10.37	155	10.27	13.9	12.9	0.66
	SDSS...	J122442.6+544441	2578	5	10	14.99					
276	CGCG...	J122536.4+502013	2563	16	4	12.12	14	9.61	5.3	2.8	2.11
	2MASX...	J122528.4+501944	2599	12	6	14.45					
277	UGC07531	J122612.0–011813	1836	42	10	12.74	29	9.11	133.5		0.71
	UM501	J122622.7–011512	1765	60	9	14.04					
278	NGC4433	J122738.6–081642	2794	10	2	9.50	79	10.95	0.0		1.42
	NGC4428	J122728.3–081004	2801	11	5	9.64					
279	ESO380–033	J122744.3–342520	2659	9	4	11.91	46	9.84	36.5		0.37
	2MASX...	J122724.9–342335	2590	74	9	12.67					
280	UGC07584	J122802.8+223516	543	5	9	13.75	39	7.72	0.0		0.40
	LSBC...	J122805.0+221727	543	5	10	14.56					
281	NGC4449	J122811.9+440540	252	7	9	7.24	36	9.49	2.0	0.6	0.37
	UGC07577	J122740.9+432944	240	5	10	10.44					
282	NGC4454	J122850.8–015621	2206	44	0	9.04	65	10.70	3.5	1.6	0.23
	CGCG...	J122850.7–020339	2254	13	4	11.71					
283	NGC4513	J123201.5+661957	2451	26	1	10.21	275	10.30	32.9		0.87
	SDSS...	J123602.3+660618	2497	58	6	13.73					
284	ESO322–031	J123648.7–420827	3236	59	-1	9.75	659	10.98	28.1		0.11

Table I: **Table.** (Contd.)

No.	Name	J2000.0	V_{LG}	\pm	T	K	R_\perp	$\log L$	$\frac{M}{L_K}$	$\frac{M^c}{L_K}$	$\log(II)$
			km s $^{-1}$			mag	kpc	L_\odot	\odot	\odot	
	ESO322–034	J123733.3–411829	3295	59	–2	9.91					
285	NGC4584	J123817.9+130635	1641	18	1	10.45	267	9.92	0.6		0.11
	IC3586	J123654.8+123112	1645	5	–1	12.11					
286	UGC07798	J123803.2–021551	2418	17	6	11.59	211	9.75	35.3	27.6	0.74
	SDSS...	J123905.8–020044	2446	5	8	14.29					
287	NGC4628	J124225.3–065816	2651	7	3	9.45	48	10.76	4.5	0.8	0.00
	NGC4626	J124225.1–070245	2718	34	4	10.94					
288	NGC4630	J124231.2+035737	556	36	10	9.88	96	9.15	68.3		0.30
	VCC1855	J124050.3+043133	586	40	1	14.48					
289	UGC07883	J124257.3–011346	3061	18	6	10.57	39	10.31	43.6	42.0	1.02
	SDSS...	J124309.6–011234	2923	13	9	15.69					
290	NGC4653	J124350.9–003340	2476	6	6	9.96	96	10.62	0.8	0.5	0.74
	NGC4642	J124317.8–003839	2494	5	4	10.36					
291	SDSS...	J124423.2+620306	2660	72	10	15.20	78	8.62	102.0		0.94
	SDSS...	J124412.1+621019	2682	8	10	15.40					
292	ESO268–044	J124842.2–450029	3233	30	3	10.59	253	10.48	26.3		0.42
	2MASX...	J124805.2–451909	3181	74	–1	11.84					
293	ESO575–012	J125147.4–221658	3367	74	4	12.47	248	9.78	520.5		0.37
	ESO575–003	J125031.7–221205	3471	74	4	13.75					
294	ESO575–017	J125240.2–221134	3223	29	7	11.60	186	10.09	3.5		0.12
	ESO575–019	J125327.9–222053	3237	5	8	12.75					
295	ESO507–036	J125259.2–240326	3138	10	4	11.22	334	10.11	114.2		0.25
	AM1251–240...	J125406.5–242538	3077	74	9	14.03					
296	NGC4793	J125440.7+285618	2474	20	5	8.48	12	10.96	3.0	0.2	1.00
	KISSR0148	J125445.2+285529	2336	67	10	15.60					
297	NGC4767B	J125445.0–395108	3241	18	6	9.79	106	10.75	15.7		0.21
	ESO323–040	J125428.5–394341	3325	74	4	12.07					
298	2MASX...	J125557.3–283846	2929	35	0	11.19	146	10.32	3.4		0.09
	ESO443–010	J125532.6–282733	2950	7	2	11.35					
299	ARK396	J125726.5–032927	2947	28	–2	10.34	133	10.41	105.8		0.42
	SDSS...	J125722.9–034028	3079	90	10	14.96					
300	NGC4830	J125727.9–194129	3142	12	–3	8.82	17	11.12	19.0	15.8	0.82
	2MASX...	J125732.7–194201	3498	74	–1	12.46					
301	UGC08127	J130103.7–015712	1297	33	10	12.68	8	8.89	0.2		0.07
	UGC08127...	J130100.7–015834	1302	5	10	13.64					
302	ESO323–068	J130157.1–410414	3103	59	3	10.32	497	10.55	63.6		0.09
	AM1300–412	J130300.4–414215	3165	74	3	11.74					
303	UGCA319	J130214.4–171415	548	8	10	11.59	40	8.53	0.8		0.84

Table I: **Table.** (Contd.)

No.	Name	J2000.0	V_{LG} km s $^{-1}$	\pm	T	K mag	R_\perp kpc	$\log L$ L_\odot	$\frac{M}{L_K}$ \odot	$\frac{M^c}{L_K}$ \odot	$\log(II)$
	UGC A320	J130316.7–172523	546	5	10	12.96					
304	LCRS...	J130235.6–113807	3293	9	4	13.14	157	9.55	2.1		0.33
	PGC045016	J130231.4–112613	3287	88	9	13.84					
305	UGC08153	J130305.9+035931	2744	5	6	10.87	47	10.12	0.4		1.65
	SDSS...	J130249.2+035836	2753	55	10	15.73					
306	NGC4961	J130547.6+274403	2528	17	6	10.84	15	10.07	0.2	0.0	1.00
	LSBC...	J130549.7+274239	2517	5	10	14.60					
307	SBS1307+542	J130908.8+535637	2608	33	3	12.13	94	9.83	11.6		1.66
	UGC08231	J130837.6+540428	2581	6	5	12.28					
308	NGC4989	J130916.0–052347	2888	38	–2	9.23	88	10.97	22.0	20.1	0.12
	NGC4990	J130917.3–051622	3029	7	–2	10.35					
309	NGC4995	J130940.7–075000	1605	7	3	8.21	402	10.94	40.6	39.7	0.02
	NGC4981	J130848.7–064639	1519	6	4	8.47					
310	NGC4988	J130954.4–430621	1842	42	–1	11.85	48	9.42	20.8		0.68
	ESO269–056	J131001.6–431243	1873	15	10	14.49					
311	UGC08246	J131004.5+341051	833	5	7	13.14	21	8.26	214.2		0.14
	MAPS–N...	J131029.2+341413	873	75	10	15.03					
312	UGC08255	J131056.5+112838	3285	6	6	11.38	184	10.16	27.7	26.0	0.20
	UGC08253	J131043.9+114228	3242	5	6	12.90					
313	ESO382–016	J131312.4–364322	3032	33	–2	9.36	164	10.92	34.2		0.38
	2MASX...	J131208.8–363934	3152	74	1	10.92					
314	UGC08316	J131406.5+480923	2619	34	4	12.49	151	9.45	94.2	69.9	1.13
	SDSS...	J131239.0+480919	2581	5	9	15.43					
315	UGC08331	J131530.3+472956	344	6	10	12.20	4	7.76	20.0		0.20
	DDO169 NW	J131518.4+473200	328	75	10	16.61					
316	IC4216	J131701.9–104612	2664	8	6	10.73	407	10.36	13.3		0.37
	NGC5066	J131828.5–101402	2639	43	1	11.20					
317	ESO576–024	J131757.5–215147	2824	75	8	13.00	169	9.55	319.9		0.65
	ESO576–023	J131739.4–213711	2749	9	8	13.13					
318	NGC5068	J131854.8–210221	471	5	6	7.51	271	9.92	7.5		0.65
	2MASX...	J132921.0–211045	457	29	–2	12.56					
319	ESO576–040	J132043.7–220304	1885	12	7	11.37	10	9.63	0.1		0.09
	[CCF97]G8	J132049.6–220318	1879	6	5	13.66					
320	NGC5144	J132254.1+703053	3325	14	5	10.07	88	10.61	9.7		0.50
	UGC08434	J132413.9+703153	3264	75	7	13.60					
321	NGC5114	J132401.7–322038	3357	26	–3	9.27	180	11.07	43.5	34.8	0.20
	ESO444–019	J132306.3–321441	3512	37	–2	10.49					
322	NGC5122	J132414.9–103915	2681	22	–1	10.02	122	10.43	26.1	24.2	0.37

Table I: **Table.** (Contd.)

No.	Name	J2000.0	V_{LG} km s $^{-1}$	\pm	T	K mag	R_{\perp} kpc	$\log L$ L_{\odot}	$\frac{M}{L_K}$ \odot	$\frac{M^c}{L_K}$ \odot	$\log(II)$
	MCG...	J132439.1–102921	2611	9	9	13.98					
323	IC4237	J132432.8–210813	2451	7	3	9.29	304	10.71	6.8		0.67
	MCG...	J132516.0–203859	2482	29	4	11.52					
324	UGC08521	J133230.8+015052	3167	6	2	10.34	164	10.46	18.3		0.81
	SDSS...	J133140.6+014800	3219	41	9	14.77					
325	2MASX...	J133549.8–341433	3086	30	4	12.82	201	9.68	234.0		0.38
	6dF...	J133536.1–343051	3017	74	5	13.06					
326	UGC08602	J133645.5+320528	3062	5	10	15.60	23	8.61	47.7	41.1	0.58
	UGC08605	J133654.3+320544	3035	5	9	15.60					
327	NGC5247	J133803.0–175303	1179	5	4	7.49	586	10.76	33.9	32.7	0.01
	ESO577–027	J134246.9–193454	1232	5	10	11.56					
328	NGC5219	J133841.7–455121	2267	45	3	9.92	255	10.35	20.5	13.2	1.15
	HIPASS...	J133928.8–461811	2306	9	8	13.83					
329	NGC5303	J134745.0+381816	1466	18	5	10.22	16	9.87	0.0		0.39
	NGC5303B	J134745.5+381533	1462	21	4	12.73					
330	ESO383–091	J135032.3–371720	857	5	7	11.02	34	9.04	121.6		1.14
	6dF...	J135113.9–372328	799	74	10	13.94					
331	NGC5342	J135125.9+595148	2368	27	1	10.14	192	10.29	18.6		0.03
	SDSS...	J134925.5+593831	2407	67	9	15.21					
332	NGC5324	J135205.9–060330	2922	5	5	9.36	122	10.78	0.7		0.29
	LCRS...	J135123.7–060413	2905	75	7	12.92					
333	IC4341	J135334.2+373120	2425	36	5	11.70	88	9.92	55.5	23.4	0.34
	UGC08795	J135248.5+372927	2359	11	6	11.96					
334	NGC5376	J135516.1+593024	2230	31	5	9.09	458	10.69	10.4		0.14
	UGC08741	J134856.3+595009	2200	45	4	11.46					
335	ESO510–013	J135504.4–264650	3262	8	1	8.79	393	11.11	12.0		1.61
	6dF...	J135543.9–261812	3320	74	5	13.06					
336	VV100	J135545.5–060010	1942	5	8	12.36	26	9.31	10.9		1.47
	VV099	J135534.2–055822	1915	52	9	13.88					
337	NGC5377	J135616.7+471408	1899	9	1	8.35	600	10.80	0.5		0.19
	SDSS...	J135005.0+462701	1905	5	9	14.85					
338	KUG1356... A	J135823.0+225317	2813	35	3	12.30	27	9.76	1.2		0.97
	KUG1356... B	J135824.7+225539	2798	35	4	12.89					
339	LCRS...	J140125.2–035816	3107	53	5	13.19	59	9.48	70.4		1.80
	LCRS...	J140115.2–035414	3162	74	5	13.94					
340	UGC08982	J140300.0+614504	1868	31	9	12.84	153	9.09	30.5		0.01
	SDSS...	J140524.6+613401	1883	5	9	14.41					
341	IC0971	J140352.8–100826	3190	5	5	10.45	58	10.46	2.8		2.26

Table I: **Table.** (Contd.)

No.	Name	J2000.0	V_{LG} km s $^{-1}$	\pm	T	K mag	R_\perp kpc	$\log L$ L_\odot	$\frac{M}{L_K}$ \odot	$\frac{M^c}{L_K}$ \odot	$\log(II)$
	IC4358	J140334.2–100904	3156	75	4	12.67					
342	ESO510–058	J140437.4–244959	2156	8	6	10.43	18	10.16	0.0		0.15
	ESO510–059	J140446.4–244938	2160	8	6	12.14					
343	UGC08995	J140447.4+084803	1182	5	8	13.18	8	8.47	42.0	38.9	0.47
	LSBC...	J140441.6+084716	1145	5	10	16.34					
344	NGC5468	J140634.9–052711	2732	5	6	10.39	55	10.57	8.7	4.6	0.49
	NGC5472	J140655.0–052738	2803	32	2	10.64					
345	HIPASS...	J140940.8–144622	2190	9	7	13.21	19	9.16	0.6		1.69
	2MASX...	J140948.6–144721	2183	74	5	13.93					
346	CGCG...	J140954.9+564921	1930	28	1	11.58	129	9.56	30.9		0.01
	SDSS...	J140942.0+563231	1903	73	5	14.11					
347	NGC5496	J141137.9–010933	1455	5	7	10.30	252	10.08	2.2		0.31
	IC0976	J140843.3–010942	1445	15	–1	10.33					
348	NGC5492	J141035.2+193644	2274	7	1	10.17	392	10.24	17.2	13.4	1.61
	FGC1717	J140953.6+201836	2299	6	8	15.03					
349	NGC5493	J141129.4–050237	2609	30	–2	8.45	616	11.04	1.5	0.3	0.21
	FGC1731	J141434.1–042502	2594	5	7	12.53					
350	NGC5526	J141353.7+574617	2180	16	6	10.32	59	10.16	42.7	42.1	0.46
	MCG...	J141312.5+574959	2274	5	9	14.36					
351	NGC5585	J141948.2+564345	458	7	7	9.49	81	9.13	20.5	13.3	0.03
	KUG1413...	J141509.3+570515	475	5	10	14.10					
352	NGC5582	J142043.1+394137	1534	20	–5	8.93	331	10.41	1.2		0.47
	UGC09242	J142521.0+393222	1525	9	7	11.73					
353	ESO385–012	J142115.7–361336	3511	7	6	11.19	258	10.38	28.7	24.5	1.00
	ESO385–014	J142224.5–360118	3464	10	4	11.86					
354	NGC5611	J142404.8+330251	2025	46	1	9.75	61	10.33	28.2	27.1	2.18
	UGC09232	J142427.3+325707	2116	5	8	13.82					
355	NGC5595	J142413.2–164323	2560	47	5	9.15	42	10.91	0.4		0.94
	NGC5597	J142427.4–164546	2534	42	6	9.89					
356	NGC5624	J142635.2+513507	2062	9	5	10.67	93	9.98	43.4	42.2	0.87
	SBS1423+517	J142524.6+513316	2123	5	9	14.13					
357	NGC5630	J142736.6+411528	2759	5	8	10.84	324	10.14	0.1		0.10
	SDSS...	J142934.1+405602	2757	34	9	14.92					
358	UGC09274	J142802.8+211814	1117	73	7	12.63	42	8.82	112.2		1.96
	UGC09282	J142841.6+212022	1155	5	10	13.36					
359	IC1014	J142818.4+134649	1277	5	8	11.36	70	9.33	0.0		1.82
	UGC09273	J142810.7+133306	1276	5	10	13.12					
360	CGCG...	J142914.5+444156	2538	46	1	11.00	306	10.09	79.8		0.34

Table I: **Table.** (Contd.)

No.	Name	J2000.0	V_{LG} km s $^{-1}$	\pm	T	K mag	R_\perp kpc	$\log L$ L_\odot	$\frac{M}{L_K}$ \odot	$\frac{M^c}{L_K}$ \odot	$\log(II)$
	UGC09251	J142631.5+445144	2486	32	6	12.45					
361	UGC09299	J142934.6–000106	1475	13	6	11.25	221	9.56	79.8		0.45
	CGCG...	J142837.8+003311	1509	19	4	12.39					
362	ESO385–031	J142931.7–343728	2921	74	6	10.61	288	10.46	40.8		0.27
	ESO385–033	J143015.7–341409	2862	5	6	11.20					
363	NGC5656	J143025.5+351915	3259	21	2	9.34	105	10.88	1.4	1.2	0.55
	SDSS...	J142950.5+352255	3288	5	6	14.64					
364	ESO511–050	J143132.6–252314	2397	8	5	10.68	249	10.10	3.3		0.90
	6dF...	J142951.5–253552	2385	74	8	13.38					
365	IC4444	J143138.6–432506	1750	6	4	8.54	85	10.65	7.2		0.66
	ESO272–012	J143101.8–431441	1694	75	9	13.63					
366	NGC5665	J143225.8+080443	2197	29	5	9.47	450	10.49	37.8		0.31
	CGCG...	J143152.5+085559	2150	39	3	12.79					
367	CGCG...	J143245.2+025454	1472	5	4	13.20	130	8.93	61.9		0.23
	SDSS...	J143235.4+031652	1490	29	5	13.31					
368	NGC5669	J143243.5+095326	1349	6	6	10.34	33	9.75	0.8		0.89
	KUG1429...	J143220.9+095560	1360	35	5	12.82					
369	NGC5612	J143401.3–782315	2458	41	2	8.92	453	10.82	18.1	15.5	1.11
	ESO022–003	J144551.0–775530	2505	7	5	12.98					
370	UGC09389	J143533.3+125430	1816	5	3	12.25	113	9.33	32.9	26.5	1.18
	UGC09394	J143539.9+131012	1793	5	6	13.40					
371	IC4468	J143826.7–222203	2310	10	5	9.83	33	10.39	8.9		0.33
	ESO580–005	J143815.9–221928	2235	74	7	13.07					
372	NGC5730	J143952.2+424432	2648	10	4	10.99	41	10.24	0.1		0.36
	NGC5731	J144009.2+424646	2643	16	7	11.55					
373	ESO447–030	J143946.3–324009	2798	23	-2	9.17	258	11.03	15.2	9.4	0.71
	ESO447–031	J144055.5–322232	2871	22	-1	9.72					
374	NGC5727	J144026.2+335921	1575	5	8	12.38	50	9.11	128.9		1.73
	SDSS...	J144003.5+340559	1522	64	10	13.87					
375	FGC1793	J144112.1–173846	3298	5	7	12.81	111	9.67	5.8	3.0	0.07
	ESO580–008	J144107.4–174707	3313	5	8	13.62					
376	UGC09504...	J144527.6+312537	1649	35	8	12.64	8	9.00	26.0	19.7	1.86
	UGC09506	J144532.6+312454	1597	5	10	14.89					
377	UGCA394	J144724.2–172644	2082	7	6	9.82	327	10.36	0.7		0.87
	ESO580–022	J144605.2–180120	2088	8	8	11.86					
378	NGC5762	J144842.6+122726	1796	5	3	10.88	187	9.78	37.8	21.1	1.29
	CGCG...	J144728.4+124554	1828	11	9	13.70					
379	SDSS...	J144948.8+362347	1979	5	10	14.20	10	8.70	0.0		1.84

Table I: **Table.** (Contd.)

No.	Name	J2000.0	V_{LG} km s $^{-1}$	\pm	T	K mag	R_\perp kpc	$\log L$ L_\odot	$\frac{M}{L_K}$ \odot	$\frac{M^c}{L_K}$ \odot	$\log(II)$
	SDSS...	J144951.1+362502	1978	32	10	14.79					
380	UGC09562	J145114.4+353232	1355	21	5	12.04	21	9.19	41.7	11.5	2.33
	UGC09560	J145056.5+353418	1305	22	9	12.79					
381	ESO512-023	J145113.8-263753	2435	6	2	9.69	9	10.57	6.9	6.7	0.79
	MCG...	J145110.4-263818	2592	15	5	11.79					
382	UGC09569	J145159.8+434314	2621	7	7	12.26	54	9.80	16.9		1.57
	UGC09567	J145146.5+433841	2662	29	6	12.41					
383	CGCG...	J145601.2+022749	2082	24	-2	11.56	191	9.62	98.5		0.46
	SDSS...	J145434.4+022038	2124	42	10	15.27					
384	NGC5798	J145738.0+295807	1870	7	9	10.94	156	10.00	4.8	2.1	0.58
	NGC5789	J145635.5+301403	1886	5	8	11.23					
385	UGC09665	J150132.5+481911	2707	7	4	10.26	82	10.38	4.0	3.3	1.11
	UGC09657	J150048.7+482139	2675	7	8	12.87					
386	IC4522	J151128.9-755136	2617	9	3	9.58	408	10.62	32.3	28.6	0.73
	2MASX...	J150622.8-751753	2670	9	6	12.56					
387	2MASXi...	J151156.7+323553	2323	5	9	14.31	89	8.83	8.6		0.16
	UGC09762:...	J151154.0+324530	2330	5	10	14.67					
388	ESO581-025	J151330.9-204030	2165	9	4	9.06	45	10.63	2.1		0.70
	2MASX...	J151338.2-204529	2124	74	5	13.34					
389	NGC5878	J151345.7-141611	1908	5	3	8.12	524	10.90	17.9	15.5	0.52
	MCG...	J151354.2-130622	1860	9	3	11.85					
390	VIZW 591	J151504.1+611212	2692	26	3	10.89	331	10.12	28.2		0.40
	MCG...	J151051.0+610852	2723	18	9	13.82					
391	NGC5899	J151503.3+420259	2726	20	5	8.57	103	11.18	4.7	4.2	0.40
	NGC5900	J151505.1+421235	2649	8	3	9.42					
392	NGC5917	J152132.6-072238	1855	36	3	10.74	32	10.04	3.8		1.19
	MCG...	J152133.3-072652	1888	75	-2	11.26					
393	MCG...	J152135.9-120536	3156	59	1	9.50	617	10.80	140.1		0.64
	6dF...	J152224.4-125219	3267	74	7	13.95					
394	MRK0482	J152804.2+553245	3515	38	2	11.19	95	10.27	8.0		0.32
	MRK0481	J152750.5+552613	3479	75	-1	13.00					
395	IC1125	J153305.6-013742	2773	12	8	10.88	76	10.14	48.7	10.4	0.30
	SDSS...	J153239.2-013606	2859	39	9	15.30					
396	NGC5957	J153523.2+120250	1871	5	3	9.48	143	10.59	23.0	22.6	0.09
	NGC5956	J153458.5+114501	1944	5	2	9.86					
397	NGC5970	J153830.0+121112	2003	5	5	8.80	67	10.73	5.3	1.7	0.09
	IC1131	J153851.7+120450	2063	26	-5	11.05					
398	ESO022-010	J153334.9-780726	2453	59	-2	10.13	444	10.53	2.2		1.17

Table I: **Table.** (Contd.)

No.	Name	J2000.0	V_{LG}	\pm	T	K	R_\perp	$\log L$	$\frac{M}{L_K}$	$\frac{M^c}{L_K}$	$\log(II)$
			km s $^{-1}$			mag	kpc	L_\odot	\odot	\odot	
	IC4555	J154814.8–781044	2465	10	6	10.64					
399	UGC09977	J154159.5+004246	1918	5	5	10.56	117	10.16	19.6	18.7	0.96
	UGC09979	J154219.5+002828	1964	5	10	10.98					
400	UGC10010	J154445.7+460441	2805	23	7	12.54	212	9.67	41.5		1.01
	MRK0490	J154630.7+455954	2832	5	9	13.09					
401	UGC10043	J154841.2+215210	2252	5	4	10.39	79	10.16	54.5		1.14
	UGC10049...	J154917.1+214943	2343	63	8	14.39					
402	NGC6015	J155125.2+621836	1041	6	6	8.47	257	10.26	50.1	48.1	0.28
	UGC10031	J154545.7+613321	1096	6	9	14.59					
403	NGC6017	J155715.5+055954	1830	75	-2	9.79	120	10.20	6.6		0.15
	SDSS...	J155614.4+060553	1857	45	9	14.70					
404	NGC6070	J160958.7+004234	2033	7	6	8.69	556	10.76	2.9	1.2	0.02
	UGC10290	J161432.9+004918	2017	6	9	11.40					
405	UGC10288	J161424.8–001227	2075	5	5	9.34	358	10.51	24.5	23.2	0.02
	VV370	J161329.0–005301	2118	5	9	12.55					
406	MCG...	J164203.2–050158	1601	5	4	8.99	383	10.46	2.2	0.6	1.42
	MCG...	J163808.6–044924	1612	5	4	11.07					
407	NGC6207	J164303.7+364957	1037	5	3	9.12	293	9.98	0.5		0.76
	UGC10477	J163734.8+371710	1033	8	7	13.25					
408	2MASX...	J164808.3–002514	2396	74	6	12.52	57	9.62	1.7		2.63
	2MASX...	J164759.2–001945	2407	9	10	12.62					
409	UGC10625	J165723.1+384019	2252	6	8	13.82	15	8.97	0.2		1.02
	SHOC553	J165730.0+384123	2255	5	9	14.37					
410	UGC10743	J171130.7+075941	2683	20	3	10.32	285	10.33	8.9	6.7	2.08
	HIPASS...	J170956.0+074713	2707	5	8	14.06					
411	UGC10770...	J171310.2+591956	1391	32	8	11.60	4	9.54	0.6		2.52
	UGC10770...	J171307.1+591924	1414	27	8	11.60					
412	NGC6368	J172711.5+113237	2905	5	3	9.13	221	10.87	0.7	0.4	0.06
	UGC10852	J172617.3+111901	2919	5	6	13.53					
413	UGC10887	J172607.0+774213	2088	5	6	12.32	185	9.57	18.3		1.84
	UGC10907	J172959.2+772347	2071	34	4	12.46					
414	UGC10864	J172819.4+141008	3030	31	-2	10.12	158	10.55	66.5	60.1	1.20
	CGCG...	J172901.7+141751	3143	16	3	12.88					
415	NGC6384	J173224.3+070337	1791	5	4	7.48	481	11.11	2.7	2.3	1.65
	UGC10862	J172808.9+072521	1816	5	5	11.66					
416	NGC6470	J174414.9+673710	1719	21	3	11.12	145	9.70	0.0		2.09
	UGC10991	J174628.9+672017	1718	5	10	12.72					
417	ESO139–049	J180035.0–590811	2611	8	6	10.25	257	10.44	40.6	36.6	0.42

Table I: **Table.** (Contd.)

No.	Name	J2000.0	V_{LG} km s $^{-1}$	\pm	T	K mag	R_\perp kpc	$\log L$ L_\odot	$\frac{M}{L_K}$ \odot	$\frac{M^c}{L_K}$ \odot	$\log(II)$
	ESO139–046	J175916.9–593026	2672	10	6	11.55					
418	NGC6548	J180559.2+183514	2369	27	1	8.55	615	11.04	15.7	10.5	0.38
	NGC6555	J180749.2+173618	2418	5	5	9.80					
419	2MASX...	J181037.5–561640	3459	36	5	10.67	92	10.65	4.5		1.15
	IC4679	J181124.5–561516	3502	16	6	10.92					
420	NGC6574	J181151.2+145854	2471	6	4	8.35	535	11.13	0.1		0.14
	NGC6570	J181107.3+140535	2466	6	9	9.82					
421	NGC6585	J181221.8+393759	3077	8	4	10.26	380	10.48	2.7	1.1	0.29
	UGC11140	J181109.3+391014	3064	5	6	13.37					
422	UGC11152	J181232.2+183556	2928	5	8	12.56	28	9.54	8.6		0.89
	UGC11152:...	J181222.5+183630	2958	20	10	15.15					
423	IC4694	J181526.4–581232	2644	9	5	10.29	265	10.60	31.6	9.8	0.88
	2MASX...	J181214.2–581503	2580	36	1	10.31					
424	NGC6599	J181543.0+245445	3253	26	-2	9.27	183	11.12	3.5		1.03
	NGC6602	J181634.3+250239	3299	25	2	9.77					
425	NGC6438	J182217.5–852407	2349	75	-2	8.22	4	11.29	0.0		0.02
	NGC6438A	J182235.5–852423	2377	75	10	8.55					
426	NGC6667	J183039.8+675913	2856	6	2	9.28	569	10.82	16.9		2.18
	UGC11222	J182156.4+680744	2897	63	6	12.32					
427	IC4721	J183424.8–582948	2116	5	6	8.90	71	10.77	45.5	45.0	1.30
	IC4720	J183332.5–582419	1936	11	6	10.00					
428	UGC11291	J183604.5+305023	3137	7	7	13.17	225	9.50	24.3		0.17
	CGCG...	J183506.2+303730	3154	29	5	13.85					
429	NGC6654A	J183927.1+733442	1824	7	7	11.91	19	9.58	1.0		0.23
	UGC11331	J183860.0+733634	1811	9	10	12.26					
430	IC4807	J190217.7–565552	3397	36	5	10.53	281	10.47	19.1	10.3	0.29
	HIPASS...	J185949.7–570128	3356	9	6	12.98					
431	NGC6764	J190816.4+505560	2700	8	4	9.33	405	10.81	2.5		1.49
	NGC6759	J190656.8+502039	2718	45	2	10.95					
432	IC4837	J191514.6–543947	2582	18	6	9.80	555	10.70	6.1		0.30
	IC4821	J190932.0–550102	2603	10	5	10.35					
433	ESO338–004	J192758.2–413432	2850	26	4	12.60	76	9.64	57.2		1.62
	ESO338–004B	J192731.6–413854	2903	75	5	13.32					
434	NGC6814	J194240.6–101925	1703	5	4	7.59	617	11.00	23.3	21.0	0.74
	HIPASS...	J194833.7–094802	1647	9	10	13.89					
435	NGC6810	J194334.4–583921	1929	46	2	8.66	86	10.68	19.6	17.9	0.19
	ESO142–032	J194236.9–584806	1833	13	10	12.88					
436	NGC6835	J195433.1–123409	1761	54	1	8.80	51	10.61	0.0		0.79

Table I: **Table.** (Contd.)

No.	Name	J2000.0	V_{LG}	\pm	T	K	R_\perp	$\log L$	$\frac{M}{L_K}$	$\frac{M^c}{L_K}$	$\log(II)$
			km s $^{-1}$			mag	kpc	L_\odot	\odot	\odot	
	NGC6836	J195440.1–124117	1763	5	9	11.11					
437	NGC6869	J200042.4+661339	3024	42	-2	8.65	679	11.08	43.8	40.3	0.74
	kkh092	J201001.1+660501	2943	11	10	14.21					
438	HIPASS...	J201046.9–113835	3352	9	7	12.28	55	9.88	75.8		0.60
	2MASX...	J201103.7–113808	3258	74	5	13.13					
439	2MASX...	J201411.8–114537	3385	74	7	11.73	276	10.05	3.0		0.60
	HIPASS...	J201252.5–113913	3395	9	5	13.29					
440	IC4960	J201523.9–703216	3324	30	-2	10.42	474	10.51	52.7	43.5	0.13
	IC4962	J201642.5–710746	3269	5	4	12.55					
441	NGC6887	J201717.3–524748	2639	8	4	8.85	117	10.89	0.3		0.63
	NGC6887:...	J201605.2–524539	2626	30	9	14.00					
442	IC1313	J201843.7–165645	3421	19	2	9.56	60	10.83	30.9	8.6	0.31
	2MASX...	J201828.6–165930	3250	74	3	12.93					
443	ESO462–025	J202908.2–275452	3127	5	8	13.28	215	9.42	203.8		0.87
	ESO462–022	J202806.0–280505	3173	68	8	14.24					
444	IC5020	J203038.5–332908	3127	8	3	9.26	91	10.88	0.1		0.18
	ESO400–037	J203113.5–332841	3119	5	6	13.72					
445	ESO596–051	J203105.0–181202	2413	74	7	11.41	3	9.89	0.0		2.74
	ESO596–051	J203106.3–181157	2414	9	8	12.87					
446	AM2029–235...	J203236.0–234258	3154	74	3	13.61	35	9.43	0.3		0.65
	AM2029–235...	J203225.5–234135	3158	74	3	13.67					
447	ESO234–049	J203518.1–495156	2536	8	4	10.59	372	10.17	7.3		0.31
	6dF...	J203210.1–493056	2520	74	9	14.23					
448	ESO186–065	J203557.2–541758	3398	26	-3	9.93	332	10.70	16.3		0.28
	IC5021	J203334.0–543115	3353	74	7	12.92					
449	ESO234–050	J203557.9–501132	2650	75	-1	11.19	125	9.96	0.1		0.31
	ESO234–056	J203702.2–500538	2648	65	8	15.91					
450	IC5039	J204314.3–295112	2763	7	4	9.88	110	10.78	0.9	0.6	0.66
	IC5007	J204334.4–294213	2783	5	7	10.09					
451	NGC6920	J204357.4–800003	2699	40	-2	8.28	75	11.13	15.6	1.4	0.36
	ESO026–005	J204601.4–800451	2545	75	9	11.40					
452	ESO285–048	J204440.2–455843	2693	5	6	10.90	173	10.13	7.5		0.32
	ESO285–051	J204600.8–455059	2715	35	9	13.28					
453	NGC6958	J204842.6–375951	2740	25	-4	8.38	138	11.11	1.6		0.21
	2MASX...	J204935.7–375240	2705	40	-3	12.39					
454	NGC7029	J211152.1–491701	2750	37	-5	8.53	702	11.06	0.0		0.55
	ESO235–073	J211157.5–502105	2750	9	8	12.79					
455	NGC7070A	J213147.3–425052	2385	26	0	9.30	198	10.80	0.2		0.59

Table I: **Table.** (Contd.)

No.	Name	J2000.0	V_{LG} km s $^{-1}$	\pm	T	K mag	R_\perp kpc	$\log L$ L_\odot	$\frac{M}{L_K}$ \odot	$\frac{M^c}{L_K}$ \odot	$\log(II)$
	NGC7070	J213025.4–430514	2392	5	6	10.01					
456	UGC11760	J213139.8+022704	3491	13	4	10.72	64	10.64	0.1		1.21
	NGC7081	J213124.1+022929	3500	9	3	10.99					
457	NGC7079	J213235.2–440403	2661	25	–2	8.57	268	11.01	23.6	10.3	0.16
	ESO287–037	J213432.0–441853	2574	33	8	12.22					
458	NGC7083	J213544.7–635410	2989	10	4	8.41	343	11.29	14.1		0.11
	ESO107–044	J214003.4–635432	3071	51	–2	9.86					
459	IC5120	J213848.3–642101	3201	10	4	10.78	336	10.30	97.8		0.12
	NGC7083a	J213506.0–641114	3271	75	9	15.82					
460	NGC7137	J214813.0+220934	1975	10	5	8.82	79	10.68	39.8	39.6	1.30
	UGC11813	J214731.1+220951	2118	5	10	14.96					
461	NGC7135	J214946.0–345235	2760	39	–3	8.84	312	11.13	21.6	11.0	0.12
	IC5131	J214725.3–345301	2671	25	–3	9.32					
462	ESO288–013	J215146.1–430725	2560	22	9	11.73	265	9.78	64.2		0.43
	2MASX...	J215356.2–431830	2525	74	5	13.51					
463	ESO027–001	J215226.4–813151	2364	5	5	9.09	74	10.70	0.4		0.27
	ESO027–003	J215345.2–813910	2378	26	10	13.74					
464	ESO404–012	J215707.2–343456	2646	26	5	9.45	274	10.81	2.4		0.15
	NGC7154	J215521.0–344851	2668	13	10	10.37					
465	UGC11866	J215834.0+140722	1970	5	4	11.80	83	9.47	6.3	3.0	2.10
	[ZBS97]A04–1	J215906.4+141421	1984	5	10	15.17					
466	NGC7177	J220041.2+174417	1424	5	3	8.14	194	10.62	17.0	16.5	1.28
	UGC11868	J215904.7+181039	1368	5	9	12.89					
467	ESO404–018	J220110.2–323444	2324	8	7	10.92	193	9.99	58.0		0.19
	6dF...	J220250.2–323437	2275	74	4	13.34					
468	NGC7168	J220207.4–514435	2702	34	–5	8.87	583	10.90	22.5		0.35
	ESO237–019	J215720.6–511303	2651	27	10	13.31					
469	ESO532–015	J220308.2–222340	1854	8	6	11.76	39	9.47	46.2	33.8	0.79
	ESO532–014	J220257.1–222819	1799	15	6	13.79					
470	AM2206–272...	J220855.9–271322	2763	37	4	11.57	52	10.04	37.7	24.5	0.44
	ESO532–022	J220911.3–270959	2681	10	6	12.08					
471	IC5169	J221010.0–360519	3062	19	–1	9.77	377	10.68	40.1		1.04
	ESO404–041	J221236.3–355730	3127	74	6	13.08					
472	ESO288–045	J221037.8–431511	2230	71	5	12.38	150	9.39	79.8		0.68
	AM2209–432	J221207.4–431038	2197	8	10	14.39					
473	2MASX...	J221247.1–254303	2756	9	3	11.91	51	9.79	0.9		0.43
	ESO532–032	J221253.2–253835	2747	5	8	13.50					
474	NGC7241	J221549.9+191356	1723	8	4	8.95	34	10.48	0.9	0.8	1.28

Table I: **Table.** (Contd.)

No.	Name	J2000.0	V_{LG}	\pm	T	K	R_\perp	$\log L$	$\frac{M}{L_K}$	$\frac{M^c}{L_K}$	$\log(II)$
			km s $^{-1}$			mag	kpc	L_\odot	\odot	\odot	
	UGC11964	J221529.1+191312	1697	5	7	12.92					
475	2MASX...	J221805.4–253116	2827	10	3	11.86	113	9.83	0.1		1.46
	ESO533–010	J221807.0–254120	2825	5	9	13.57					
476	NGC7259	J222305.5–285717	1789	37	3	10.75	21	9.83	29.1	27.6	1.31
	ESO467–051	J222316.4–285848	1879	8	6	14.21					
477	MCG...	J222741.5–094337	1786	43	8	13.10	33	9.08	208.3		2.64
	6dF...	J222730.5–093959	1866	74	9	13.59					
478	NGC7307	J223352.5–405558	2088	5	6	10.41	158	10.12	113.5		0.95
	ESO345–027	J223414.4–411404	2178	75	8	12.85					
479	NGC7314	J223546.2–260301	1511	5	4	8.18	99	10.67	1.2	0.9	1.45
	ESO534–001	J223607.0–261852	1490	5	9	13.33					
480	ESO534–010	J223851.6–254233	3207	42	–3	9.94	371	10.62	71.3		0.27
	ESO534–015	J224000.8–260728	3125	74	2	14.18					
481	ESO534–021	J224434.7–225931	3247	13	5	11.65	314	10.08	5.6		0.36
	2MASX...	J224419.6–232329	3261	31	7	12.82					
482	NGC7416	J225541.7–052943	3031	10	3	9.23	654	10.86	12.0		1.85
	MCG...	J225834.5–045618	2998	74	6	13.82					
483	IC5273	J225926.7–374210	1310	9	6	8.75	164	10.31	21.6	20.1	0.27
	ESO406–040	J230022.2–371205	1263	6	10	14.15					
484	NGC7448	J230003.6+155849	2449	6	5	8.99	317	10.79	6.5	5.9	0.05
	UGC12321	J230219.0+160140	2417	5	4	12.07					
485	NGC7457	J230059.9+300842	1119	11	–3	8.17	36	10.46	12.7	12.3	0.32
	UGC12311	J230125.1+301421	1211	8	6	12.34					
486	NGC7456	J230210.4–393410	1212	8	6	9.35	310	10.03	4.2		0.35
	LCRS...	J230153.2–382941	1201	30	10	12.31					
487	ESO027–021	J230419.1–792757	2308	20	1	10.56	46	10.13	8.4	6.2	0.74
	[SOM2000]...	J230415.6–793258	2262	10	9	12.75					
488	UGC12347	J230512.2+185205	1899	21	10	12.32	78	9.43	0.7		0.29
	UGC12344	J230460.0+184212	1895	5	8	12.80					
489	NGC2573B	J230732.8–890659	2311	24	10	12.06	12	9.70	0.8		0.75
	NGC2573A	J231227.2–890734	2328	75	3	12.60					
490	NGC7541	J231443.9+043204	2894	8	5	8.33	37	11.25	0.0		1.11
	NGC7537	J231434.5+042954	2893	5	4	10.19					
491	NGC7625	J232030.1+171332	1878	8	1	8.86	177	10.60	0.5		0.50
	UGC12549	J232153.5+172612	1888	5	10	13.52					
492	ESO536–003	J232216.0–234204	1774	75	6	13.58	62	8.79	627.0		1.73
	2MASX...	J232217.9–233306	1702	74	8	14.51					
493	NGC7667	J232423.1–000629	2892	7	9	12.22	15	9.64	1.6	1.1	1.52

Table I: **Table.** (Contd.)

No.	Name	J2000.0	V_{LG} km s $^{-1}$	\pm	T	K mag	R_\perp kpc	$\log L$ L_\odot	$\frac{M}{L_K}$ \odot	$\frac{M^c}{L_K}$ \odot	$\log(II)$
	UM160e	J232423.4–000514	2912	6	10	16.15					
494	NGC7637	J232627.7–815442	3447	55	5	9.60	31	10.83	33.8	32.7	1.42
	ESO012–001...	J232555.4–815241	3195	16	5	12.02					
495	UGCA439	J232632.8+181560	1834	60	9	12.78	137	9.01	828.7		0.50
	EXG...	J232554.1+183245	1762	75	9	15.66					
496	NGC7676	J232901.7–594300	3250	35	-3	9.39	410	10.88	70.0		0.31
	ESO148–009	J232456.9–594720	3354	74	5	13.31					
497	ESO148–017	J233006.7–592753	2995	21	-5	9.48	559	10.78	37.3		0.31
	ESO148–014	J232729.2–600952	3053	74	3	12.61					
498	NGC7694	J233315.8–024210	2461	5	10	10.77	10	10.14	3.3		0.01
	NGC7695	J233315.0–024313	2400	75	2	12.35					
499	ESO291–034	J233522.2–425332	3186	9	4	11.63	351	10.12	54.5		0.58
	2MASX...	J233331.0–423441	3144	74	1	12.28					
500	NGC7712	J233551.6+233707	3319	5	2	10.47	383	10.53	4.5	3.2	1.67
	UGC12675	J233438.3+231328	3301	5	4	12.00					
501	NGC7714	J233614.1+020919	3000	9	3	9.74	24	10.66	1.0	0.4	0.95
	NGC7715	J233622.1+020924	2960	16	9	12.70					
502	ESO240–010	J233743.6–473013	3143	45	-2	8.65	302	11.20	14.6	11.2	0.16
	ESO240–013	J233927.0–474629	3223	10	3	10.63					
503	NGC7721	J233848.6–063104	2173	5	5	8.67	404	10.81	8.8	5.0	0.23
	MCG...	J233848.9–054448	2208	11	9	12.60					
504	NGC7731	J234129.1+034424	3084	11	1	10.62	19	10.59	0.2		0.55
	NGC7732	J234133.9+034330	3104	17	7	10.77					
505	NGC7741	J234354.4+260432	1017	5	6	9.61	181	9.77	0.1		0.31
	UGC12732	J234039.9+261411	1016	5	8	13.35					
506	NGC7751	J234658.3+065142	3456	9	0	9.60	25	10.80	18.4	18.3	1.48
	ESDO...	J234650.7+065131	3259	6	10	14.13					
507	NGC7755	J234751.8–303119	3001	7	5	8.96	285	10.95	21.4	7.7	0.78
	APMUKS...	J234650.7–301105	2926	30	9	15.63					
508	ESO472–006	J235404.5–252716	3091	40	9	11.74	102	10.01	0.4		0.37
	APMBGC...	J235440.2–252919	3085	26	5	12.77					
509	NGC7793	J235749.8–323528	247	10	7	6.85	165	9.59	29.6	5.7	0.53
	ESO349–031	J000813.4–343442	223	11	10	13.41					

Acknowledgments

This work was supported by the Russian Foundation for Basic Research (grant nos. 07-02-00005, 08-02-00627, and 07-02-00792) and the joint grant (no. 06-02-04017) of Deutsche Forschungsgemeinschaft and Russian Foundation

for Basic Research. We acknowledge the use of the HyperLeda database (<http://leda.univ-lyon1.fr>) and NASA/IPAC Extragalactic Database (NED) (<http://nedwww.ipac.caltech.edu/>). We thank V. E. Karachentseva for finding the magnitudes and types for a large number of dwarf galaxies.

-
- [1] I. D. Karachentsev, V. E. Karachentseva, W. K. Huchtmeier, and D. I. Makarov, *Astronom. J.* **127**, 2031 (2004).
 - [2] I. D. Karachentsev, *Astronom. J.* **129**, 178 (2005).
 - [3] I. D. Karachentsev, V. E. Karachentseva, W. K. Huchtmeier, et al., in *Proceedings of the Galaxies in the Local Volume, Sydney, 2007*, Ed. by B. Koribalsky and H. Jerden (2008).
 - [4] R. B. Tully, *Astrophys. J.* **321**, 280 (1987).
 - [5] R. B. Tully, *Nearby Galaxy Catalog* (Cambridge Univ. Press, 1988).
 - [6] R. B. Tully and J. R. Fisher, *Astronom. and Astrophys.* **54**, 661 (1977).
 - [7] R. B. Tully, E. J. Shaya, I. D. Karachentsev, et al., *Astrophys. J.* **676**, 184 (2008).
 - [8] J. P. Huchra and M. J. Geller, *Astrophys. J.* **257**, 423 (1982).
 - [9] A. C. Crook, J. P. Huchra, N. Martimbeau, et al., *Astrophys. J.* **655**, 790 (2007).
 - [10] J. Vennik, *Tartu Astron. Obs. Publ.* **73**, 1 (1984).
 - [11] I.D. Karachentsev, *Astron. and Astrophys. Trans.* **6**, 1 (1994).
 - [12] A. Sandage, *Astrophys. J.* **307**, 1 (1986).
 - [13] E. F. Bell, D. H. McIntosh, N. Katz, and M. D. Weinberg, *Astrophys. J. Suppl.* **149**, 289 (2003).
 - [14] M. Fukujita, T. Ichikawa, J. Gunn, et al., *Astronom. J.* **111**, 1748 (1996).
 - [15] I. D. Karachentsev and A. M. Kut'kin, *Pis'ma Astronom. Zh.* **31**, 299 (2005).
 - [16] I. Broelis, *Dark and Visible Matter in Spiral Galaxies*, PhD Thesis (Groningen, 1992).
 - [17] R. A. Swaters, T. S. van Albada, J. M. van der Hulst, and R. Sancisi, *Astronom. and Astrophys.* **390**, 829 (2002).
 - [18] A. Begum, J. N. Chengalur, and I. D. Karachentsev, *Astronom. and Astrophys.* **433**, 1 (2005).
 - [19] J. Guzik and U. Seljak, *Monthly Notices Roy. Astronom. Soc.* **335**, 311 (2002).
 - [20] G. Paturel, C. Petit, P. Prugniel, et al., *Astronom. and Astrophys.* **412**, 45 (2003).
 - [21] I. D. Karachentsev, D. I. Makarov, V. E. Karachentseva, and O. V. Mel'nyk, *Pis'ma Astronom. Zh.* (2008) (in press).
 - [22] G. de Vaucouleurs, A. de Vaucouleurs, and H. Corwin, *Second Reference Catalogue of Bright Galaxies* (Texas, Austin, 1976).
 - [23] T. N. Jarrett, T. Chester, R. Cutri, et al., *Astronom. J.* **119**, 2498 (2000).
 - [24] T. N. Jarrett, T. Chester, R. Cutri, et al., *Astronom. J.* **125**, 525 (2003).
 - [25] A. Bizzoni, *Monthly Notices Roy. Astronom. Soc.* **361**, 725 (2005).
 - [26] M. Fukujita, K. Shimasaku, and T. Ichikawa, *Publ. Astronom. Soc. Pacific* **107**, 945 (1995).
 - [27] V. E. Karachentseva and I. D. Karachentsev, *Astronom. and Astrophys. Suppl. Ser.* **127**, 409 (1998).
 - [28] V. E. Karachentseva and I. D. Karachentsev, *Astronom. and Astrophys. Suppl. Ser.* **146**, 359 (2000).
 - [29] D. J. Schlegel, D. P. Finkbeiner, and M. Davis, *Astrophys. J.* **500**, 525 (1998).
 - [30] J. Heisler, S. Tremaine, and J. N. Bahcall, *Astrophys. J.* **298**, 8 (1985).

- [31] J. Binney and M. Merrifield, *Galactic astronomy*, (Princeton University Press, Princeton, 1998).
- [32] A. P. Magtesian, *Astrofizika* **28**, 150 (1988).
- [33] E. Gourgoulhon, P. Chamaraux, and P. Fouque, *Astronom. and Astrophys. Suppl. Ser.* **225**, 69 (1992).
- [34] H. Arp, *Astrophys. J.* **256**, 54 (1982).
- [35] J. N. Chengalur, S. A. Pustilnik, J. M. Martin, and A. Yu. Kniazev, *Monthly Notices Roy. Astronom. Soc.* **371**, 1849 (2006).
- [36] B. B. Tully, L. Rizzi, A. E. Dolphin, et al., *Astrophys. J.* **132**, 729 (2006).
- [37] I. D. Karachentsev, *Binary Galaxies* (Nauka, Moscow, 1987) [in Russian].
- [38] L. Reduzzi and R. Rampazzo, *Astrophys. Lett. and Communic.* **30**, 1 (1995).
- [39] Ekta, J. N. Chengalur, and S. A. Pustilnik, *Monthly Notices Roy. Astronom. Soc.* **372**, 853 (2006).
- [40] K. Bekki, [astro-ph/0805.0662](#)